BYPASS TRANSITION TO TURBULENCE AND RESEARCH DESIDERATA

Mark V. Morkovin
Illinois Institute of Technology
Chicago, Illinois 60616

Bypass transitions are seldom mentioned in texts or meetings on instability and transition to wall turbulence. Like poor relations, they are untidy; they spoil the beautiful orderly structure of instability theories and devalue our rational tools for improved understanding of the onset of turbulence in boundary layers, pipes, and ducts. I shall first try to illustrate the nature of a number of bypass transitions by examples. Like a Sunday preacher, I will use visualizations of concrete phenomena to have something to preach about and to convey a physical feeling for the associated mechanisms whenever possible.

HISTORIC BYPASS - THE BLUNT-BODY PARADOX

Turbulent wedges on blunt noses (fig. 1) was the first class of bypass identified (ref. 1). The fact that transition occurred very early on many spherical noses was a shock to designers of reentry vehicles in 1957. All theories said that the accelerated cooled boundary layer was stable, and yet flight tests (ref. 2) showed transition on the nose for laminar Reynolds numbers based on the momentum thickness Re_θ of the order of 100 to 200. Two multimillion dollar contracts based on copper heat sinks "melted away" with this finding of high turbulent heat transfer. Tens of millions of dollars were lost because the path to turbulence bypassed all known theories. Ten years later I coined the word "bypass" to describe this "blunt-body paradox" and to drive home to designers that we cannot trust stability theory alone. Predicting transition, without allowing for bypasses, remains risky. To this day, the mechanism of the early transition on blunt bodies remains unexplained. Many classes of bypass, as Bob Graham described in the Introduction, are due to large disturbances, but there are no clearly large disturbances evident in the blunt-body paradox. I found wall roughness to be the most likely contributor to the phenomenon (ref. 3, sections III-6 and III-9). When the mirror finish on NASA Lewis test vehicles (protected by plastic sheets up to the test altitudes) did not keep the roughness below 5 ?in rms, a bypass occurred. Even 10-?in roughness is very small (not truly measurable by most mechanical profilometers); yet it was in some sense excessive for the thin boundary layers in the given flight disturbance environment. Until we truly understand why this is so, predicting transition on the basis of theory or statistically inadequate correlations (as they all are) entails risks that should be considered in justifying any design involving transition.

CONCEPT OF MINIMUM REYNOLDS NUMBER FOR SELF-SUSTAINING WALL TURBULENCE AND LATERAL CONTAMINATION

Figure 1 also illustrates the concept of the turbulent $Re_{\theta,min}$. To me, a most important concept is that at certain low Reynolds numbers a temporarily turbulent boundary layer cannot sustain itself. If made turbulent through forced local separation, it relaminarizes. Relaminarization in accelerating boundary layers on smooth spheres or cylinders is known to occur within 15° to 20° from the stagnation point, at least for the Reynolds number based

on the diameter of the sphere or cylinder Re_D in the range 3×10^4 to 3×10^5. Sustenance of turbulent "bursting" processes near the wall is the crucial feature. A vehicle returning from a Mars mission must remain below $Re_{\theta,min}$ or carry extra weight in retrorockets and their fuel so as not to burn up in Earth's atmosphere. One of the most important results that should come out of any bypass transition research is consistent identification of $Re_{\theta,min}$ for the different boundary-layer classes.

In flat-plate boundary layers (fig. 1) disturbances were introduced (refs. 4 and 5) through large isolated roughnesses or sparks. One of the primary effects of such large disturbances is local boundary-layer separation, which brings about highly unstable inflectional profiles. An early transition on an inflectional profile may or may not grow. It may relaminarize after reattachment as already mentioned. The non-Blasius boundary layer may sustain turbulence in the narrow wake (fig. 1). The wake diverges slowly and parabolically, as a turbulent diffusing wake will do when the boundary layer next to it remains completely laminar and stable. At some stage the neighboring Blasius layer, the boundary layer in which we are interested, suddenly "allows" the turbulence to spread along a turbulent wedge-front, making an angle of 8° to 11° with the streamwise direction. The beginning of the wider spreading locates $Re_{\theta,min}$ empirically. The spreading is called transition by transverse or lateral contamination. Note that there is nontrivial uncertainty in pinpointing this location - a matter of subjective judgment. For the flat plate this location coincides very nearly with that of the Tollmien-Schlichting-Schubauer (TS) critical Reynolds number Re_{cr} for the growth of infinitesimal disturbances. This was noticed by Dr. H.L. Dryden some 9 years before he became head of NASA. We then have a large disturbance and yet its initiation of turbulence in a Blasius layer coincides with the infinitesimal instability criterion. We now know that this happens to be a coincidence, though it is still not understood.

FLOWS WITH KNOWN $Re_{\theta,min}$ AND Re_{cr}

On spheres and circular cylinders Re_{cr} and $Re_{\theta,min}$ have a completely different relationship: $Re_{\theta,min}$ can be substantially below Re_{cr}. Because of the pressure gradient my conjecture is that $Re_{\theta,min}$ depends on Re_D - all unexplored research territory. For pipe flows Re_{cr} is infinite, whereas Re_D for self-sustained wall bursting in so-called turbulent slugs (ref. 6) is about 2700. (The flow confinement in pipes makes possible a different mode of steady self-sustenance of turbulence at an Re_D of about 2200, the puff turbulence (ref. 6); this turbulence is presumably sustained by self-perpetuating inflectional instability taking place away from the wall.) In two-dimensional Poiseuille duct flows Re_{cr} based on half of the distance between the parallel plates is approximately 5770; growing and convecting turbulent patches, however, arise spontaneously (ref. 7) at the low Re of about 1500, the effective minimum Reynolds number. The nature of this transition remains unknown - another bypass. The physical confinement enhances the role of unsteady pressure fluctuations, which spread elliptically in all directions at large effective rates.

One unconfined boundary layer also maintains constant thickness and therefore constant Re_θ all along its length: the boundary layer along the attachment lines on a swept wing of constant chord or on an inclined long cylinder. For such attachment layers $Re_{\theta,min}$ is approximately 100 (ref. 8), whereas the critical Re_θ is 236 (ref. 9). Forced turbulent

spots at Re_θ below 100 relaminarize as they travel along the blunt leading edge; clearly this information is relevant in turbomachinery.

The information in the preceding paragraph essentially exhausts our knowledge concerning $Re_{\theta,min}$. Before we go on to other types of bypass, we should comment on an assumption that is often hidden in the experimental accounts. Since we are dealing with self-sustenance of turbulence, the momentum thickness θ should refer to the nonintermittent, turbulent boundary layer at the given location x. We can often measure or at least compute with some degree of assurance the laminar velocity profile, and hence θ_{lam}, as a function of x but not the new turbulent profile. If a laminar profile were to turn turbulent "instantaneously" at the given x, without the intervention of a drag-producing element, θ_{turb} would equal θ_{lam}. All of the $Re_{\theta,min}$ values quoted above are understood in this sense. A useful discussion of the relation between contiguous laminar and turbulent boundary layers and of transition tripping devices is due to Preston (ref. 10). Finally, we should observe that the mechanism of lateral contamination is distinct from the mechanism that originally caused the turbulence. Lateral contamination by turbulent wedges or intermittent turbulent spots in boundary layers therefore represents a separate bypass mode that can be present anywhere downstream of $Re_{\theta,min}$. There is no theory nor even a crude model for, say, the angle of lateral contamination as a function of pressure gradient and Mach number. At supersonic speeds it can be as low as 5°.

BROAD CLASSIFICATION OF LARGE DISTURBANCES

Large "disturbances" that can cause bypass transition in otherwise smoothly developing boundary layers can be steady or unsteady and can originate in the oncoming stream or at the body surface. One way to look for the potential causes of bypasses of all established stability theories is to ask what features make possible the analysis of the instability mechanisms besides the presence of small disturbances. Invariably the base flows that are perturbed to study the instabilities are characterized by dependence on a minimum of independent variables (x, y, z, and t) and other parameters such as wall curvature and sweepback. The smoothly distributed vorticity $\vec{\omega}$ of the base flow is generally oriented along a single coordinate, spanwise or azimuthal (in axisymmetric shear layers). The perturbations of the nonlinear vorticity-rotating and -stretching source term $\vec{\omega} \cdot grad(\vec{V})$ in the vorticity equation is then absent from the linearized perturbation equations. The associated powerful inviscid vorticity-generating mechanism thus remains inoperative in the first (primary) instability. If, however, there is a sufficiently large steady deformation of the wall or if a sufficiently large steady secondary flow or shear layer in the stream such as a wake from an upstream stator interacts with the boundary layer, the base flow possesses a three-dimensional $\vec{\omega}$ to start with. When we perturb these flows, the extra vorticity-generating mechanism is then present in the primary instability and is likely to lead to an earlier transition. The steady large disturbances would cause a bypass of the known, analyzed instability patterns.

Similarly a large unsteady disturbance can make the base flow temporarily highly unstable. If the instability is very fast, it may be completed before the original large disturbance runs its course and thus generate a bypass. Inflectional instabilities and the rotate-stretch mechanism in particular can be very rapid in many practical situations.

The distributed vorticity in the base flow may be likened to an amplifier system. Steady and unsteady large disturbances can redistribute the vorticity enough to make the amplifier act more powerfully and in new modes not excitable in the original amplifier system. In the examples given, the large disturbances did just that. Besides acting in this role of a modifier of the amplifier system, large disturbances invariably provide direct input into the amplified signal, higher in intensity and richer in spatiotemporal spectral content. This is also the role assigned to the "environment" in small-disturbance theory. Unsteady potential pressure gradients (including sound), entropy, and vorticity fluctuations and nonhomogenities in the stream can all induce unstable vorticity eigenfunctions in boundary layers through many mechanisms broadly called receptivity. Linearized quantitative theories of receptivities to the different stream disturbances are currently under development.

The increased intensity of the disturbances should make the same primary instabilities develop faster and farther upstream. This is important even though not strictly a bypass behavior. However, finite amplitudes should open up additional threshold-dependent instabilities in the "enlarged amplifier system." Many interactive instabilities (ref. 11), which are relegated to secondary instabilities in small-disturbance environments, may emerge as primary instabilities and alter the path to turbulence. Admittedly, many of these possibilities are speculative, simply because no reliable studies have been reported on the instability characteristics in boundary layers forced by large three-dimensional disturbances, in which at least two of the three rms fluctuation levels u', v', and w' exceed 3 percent of the mean free-stream velocity U_e. If we compare these 3-percent magnitudes to those present at the onset of turbulence in a Blasius layer at the Herbert breakdown (ref. 11), we can appreciate better the possibilities of interactive instabilities. These latter disturbances correspond roughly to a u'_{max} of the fundamental TS wave of the order of $0.01 U_e$ and to similar amplitudes of the resonant skew subharmonic and of the rest of the broadband spectrum. Since rms fluctuations add in the square, the forcing large disturbances with nonresonant $u' \approx 0.03$ U_e exceed the disturbances in observed cases of incipient turbulence. Herbert's interaction can begin at levels of the fundamental $u' \approx 0.006 U_e$ and the subharmonic at $u' \approx 0.0006 U_e$. In view of such indirect information the likelihood of interactive instabilities becoming primary appears quite plausible. Mentioning such possibilities is intended primarily to stimulate the imagination of those embarking on research into large disturbances, and not as a prediction.

LARGE WALL DISTORTIONS AND HORSESHOE VORTICES

We have established that large disturbances, steady or unsteady, at the body surface or in the stream, enhance and modify the vorticity-amplifying system and in addition supply more intense and spectrally richer fluctuations, which are amplified. Let us go back to the visual evidence of concrete examples; we start with strong disturbances due to wall deformation - a more detailed elaboration of the phenomena leading gradually to the top pattern of figure 1 - and continue with even stronger disturbances. The motivation for the choice of this example is multiple. First, the fixity of wall deformations makes evident many modes of vorticity behavior that cannot be easily photo-graphed and analyzed when the strong disturbances are convected with the stream. Second, a very damaging disturbance in turbomachinery is associated with a horseshoe vortex formed at the intersection of the blades or vanes with the hub or casing wall. Our example deals with a circular cylinder that

protrudes to an increasing height k into and ultimately through the laminar boundary layer of thickness δ. Since smoke tracers do not penetrate into all of the regions of interest, we shall precede the photographs with two complementary sketches of the flows of interest (figs. 2 and 3) due to Gregory and Walker (ref. 12) and to Charles R. Smith of Lehigh University. These sketches are based on numerous observations, with different tracers introduced at different locations, and represent a consensus of most observers.

To my knowledge the Gregory-Walker sketch is historic; it gave the first three-dimensional topography of separated flow around a three-dimensional protuberance. Also, as a result, our intuitive concept of separation, nurtured by quasi-two-dimensional textbook examples, requires revision to allow for throughflow and partial openness of the "local pockets of separation": the separation surface has "inlets" and "exits." A central-plane streamline, just above that shown approaching the protuberance in figure 2(b), comes to a stagnation point S', where the highest pressure is experienced on the surface of the obstacle. Pressure gradients on the obstacle from S' toward the wall propel the rollup of the open slice of the vortical boundary layer from the wall to the dividing stream surface, which has S' as its high point. The resultant horseshoe vortex H diverts the initial ω_z vorticity into the two spiraling vorticity tubes oriented in the x direction. The slice of the oncoming boundary layer above the dividing stream surface through S' forms the side and top shear layers, which are stable at the low Reynolds number portrayed here. In steady flow these shear layers effect an incomplete closure of the near wake along a higher pressure dashed line through S at the wall, a very complex rear singularity. The top rear surface of this steady three-dimensional separation pocket is pierced by a steady outflow in the form of two weak spiral vortices (evident in all three projections). The inflow into the slowly recirculating rear "separated" region comes partly from the inner segments of the side and top shear layers and partly through two symmetric back openings in the wall (figs. 2(a) and (b)). The two arms of the horseshoe vortex tube lift off the wall as they are forced to rotate around the obstacle and open two symmetrically located "inlets."

The Reynolds number Re_k that governs the flow around obstacles is defined as $(U_k k)/v$, where U_k is the boundary-layer velocity at the obstacle height k in the absence of the obstacle and v is the dynamic viscosity. The complicated flow described above and depicted in figure 2 is stable at Re_k of 300 to 450, depending on the shape of the obstacle and the pressure gradient along the wall. As far as we know, all symmetric protuberances at low Reynolds numbers have flow fields topologically similar to that depicted in figure 2. These flows are the base flows that would have to be perturbed if we were to study their stability analytically. At present not even advanced computers can resolve such details of the base flows as the spiral vortices and the wall inlets. The resulting instabilities will have to be specified empirically. Because of the complex flow geometry they bypass previously analyzed patterns. Here we are following the visual evidence to obtain a "feel" for what can happen in fields generated by large disturbances.

TRANSITION CAUSED BY ISOLATED THREE-DIMENSIONAL EXCRESCENCES

As Re_k grows past 300 to 450 (depending on obstacle shape) the weak top spiral vortices strengthen and begin to weave closer and closer to the rear separating surface. With rising Re_k the separating surface becomes unsteady and soon sheds periodic intertwined hairpin vortices (fig. 3). Lift is exerted

on the hairpin loops by the boundary layer, and the loops move toward the edge of the boundary layer as they are convected downstream. Norman (ref. 13) measured local u'/U_e as high as 0.04 at distances 30k to 40k (k = height length) downstream of the protuberance without any subsequent instability that would render this complex periodic flow turbulent. Under these conditions the pattern decays and transition occurs far downstream, usually through primary TS and subsequent secondary and tertiary instabilities. There is, however, some evidence that the far wake of the large disturbance caused by the pro-tuberance contributes to a somewhat earlier growth of the TS and secondary instabilities.

As Re_k reaches 550 to 650, depending on the shape of the obstacle, with x_k past Re_{cr}, the transition starts moving upstream very rapidly. An increment of 20 in Re_k may halve the $x_{tr,0} - x_k$ distance to transition. This rate decreases as x_{tr} approaches x_k asymptotically. As we shall see shortly, transition will remain near the obstacle although new instabilities will appear as Re_k increases. The nature of the instability that brings on the rapid forward movement of x_{tr} is currently being investigated by P. Klebanoff. It bears resemblance to the final instability in the transitions commencing with TS waves as the primary instability. The final "burst" takes place near the wall, probably as an interaction of the horseshoe vortex and the intert-wined legs of the hairpin vortices; stretching of these legs by convection and lifting of the loops (fig. 3) should provide extra intensification.

In figure 4(a), due to Norman (ref. 13), x_{tr} is far downstream of the protruding cylinder. Any smoke that may have penetrated the wake was diffused by the motions of the hairpin loops of figure 3. The horseshoe vortex is clearly upstream of the cylinder; downstream, along the inner edge of the arms of the horseshoe vortex, weak periodic undulations indicate the influence of the unseen loops. In figure 4(b), the interaction with the moving hairpin vortices is clearly visible at the inner boundary of the horseshoe vortex tubes. The wake spreading is still parabolic, but x_{tr} must be approaching the downstream end of the photograph. In figure 4(c), turbulence starts near the end of the separation and spreads along a nearly straight turbulent wedge front, as discussed in connection with figure 1(a).

In figure 4, Re_k was changed by increasing U_e and keeping the height constant and equal to the diameter of the cylinder. Except for figure 4(c), Re_{cr} was downstream of x_k. In figure 5, the height k and the cylinder diame-ter were increased in a constant boundary layer, keeping k/D equal to unity. In figure 5(a), the larger disturbance of the cylinder protruding through the boundary layer is seen to generate two additional horseshoe vortices upstream of the cylinder. Simultaneously, we witness the appearance of a new type of instability on the inner horseshoe. This spiral instability now governs the transition to turbulence as its dominant factor. But the horseshoe vortices begin to oscillate as Re_k is increased. Configurations of four horseshoe vortices collapsed periodically, as if the inner one broke and convected away, while the others moved up by one, an occurrence labeled "burping." Three-vortex configurations burped occasionally, presumably because of larger random modulation of free-stream disturbances, which must introduce the unsteadiness into fixed-obstacle instabilities. This behavior is probably present in the horseshoe vortices formed at the intersection of the blades or vanes with the hub or casing wall in turbomachinery. If the configuration burped, letting loose some fluid that was next to the wall and replacing it with fresh fluid, a condition of high heat transfer would be created. Unsteady motion at the

equivalent of the stagnation point S' in figure 2(b) also generates high
local heat transfer. This is compounded by intersecting shock waves at super-
sonic and hypersonic speeds; special tailoring of local geometry is needed to
protect the roots of control fins on high-speed vehicles operating at lower
altitudes.

In figure 5(c), the disturbance is so strong that transition actually
occurs on the horseshoe vortices as they form in front of the obstacle. There
is little probability that such instability and transition can be handled with
confidence computationally for decades. All of the preceding illustrations of
bypass transition were for relatively low Reynolds numbers for two reasons.
First, bypasses are expected to occur at the lower Reynolds numbers between
Re_{cr} and $Re_{\theta,min}$ (if these can be estimated). Second, we are able to
observe the otherwise undescribable complexity of the motions and the multi-
plicity of instabilities and thus acquire some "feel" for what may be in store.

At higher body Reynolds numbers these events will move toward the leading
edge and be lost to the resolution of our visualization techniques. Neverthe-
less, to the extent that we have accounted for the dominant characteristic
length and velocity scales, we can extrapolate the present lessons to practical
situations, at least qualitatively, through the appreciation for the mechanisms
that may be involved. Such appreciation is a prerequisite for designing of
meaningful experiments in the realm of large disturbances.

We may ask what would happen in these cases of large wall disturbances if
we added stronger free-stream turbulence. It depends on whether the local
flows in figure 4 can sustain turbulence once it is triggered; in other words
are the flows in the horseshoe vortex and at the separation surface above their
own Re_{min}? Since these flows already have three-dimensional vorticity and
locally inflectional profiles, the turbulence might be sustainable in figures
4(a) and (b) without propagating into the neighboring laminar layer by lateral
contamination as occurred upstream of Re_{cr} in figure 1(a). The local heat
transfer at the obstacle would then rise substantially. If in the case of
figure 4(a), say, Re_{min} were not reached, the heat transfer in the presence
of higher free-stream disturbances would rise much less because it would remain
governed by laminar conduction scales. The additional unsteadiness imposed by
the external free-stream turbulence is then likely to bring about a second-
order effect.

EFFECT OF A WAKE IMPINGING ON A BLUNT BODY

Let us now consider what lessons we can draw from a few experiments with
moderate disturbances coming from the free stream toward a body without the
disturbing wall deformation just discussed. For larger stream disturbances the
region of concern is usually the leading edge, especially when the oncoming
fluid is hot, whether in propulsive and cooling devices or downstream of a
strong shock in supersonic flight. Figure 6, due to Hodson and Nagib
(ref. 14), shows schematically how a low-Re wake from an upstream cylinder of
diameter d causes a pair of horseshoe vortices in the stagnation region of a
circular or rectangular cylinder of breadth D. In 1973 it occurred to me that
a momentum defect in a stream impinging at right angles to the stagnation line
S_{ℓ}-S of a two-dimensional body should generate horseshoe vortices just like the
momentum defect in a boundary layer does as the high-pressure region of the
protruding cylinder is approached in figure 4. The next day Nagib and Hodson
produced visual evidence of the phenomenon and later went on to document its

nonlinear onset and its implication for heat transfer. The stagnation pressure along S_ℓ, on the sides of the wake, induces flow down the pressure gradient toward the full stagnation point at S. When the pressure at S exceeds sufficiently the stagnation pressure associated with the streamline of least momentum, such as that leading to S_f, there is counterflow and horseshoe vortex formation. (See also Morkovin (ref. 15) for a detailed discussion of theoretical and experimental evidence of instabilities in stagnation regions and the empirical threshold curve for the vortex formation of Hodson and Nagib.)

One of the Hodson-Nagib dye visualizations in water of the vortex pair in front of the flat face (dark vertical line on left) is shown at the top of figure 7. The horizontal dye line marks the center of the steady laminar wake of a rod at $Re_d = 30$; the body Reynolds number $Re_D = 1040$ has only secondary influence. Heat can be carried to and from the body on a large nonmolecular scale, and its transfer has local spanwise maximums and minimums. These can be quite high and could cause local damage. In steady flow the spatially averaged heat transfer along the leading edge appears to be of second order, according to Hodson and Nagib (ref. 14).

UNSTEADY EFFECTS AND HEAT TRANSFER

The average heat transfer increases with unsteadiness. In the lower half of figure 7 where $Re_d = 365$ and the wake is weakly turbulent, horseshoe vortices are still forming but they dance back and forth. The blue dye (B) and the yellow dye (Y) originate far upstream and pass just below and above the wake-generating rod. Despite the turbulence and slight three-dimensionality of the wake, both dyes are drawn into the two-dimensional "mushroom" from the region of high stagnation pressure, as suggested in the lower half of figure 6.

Figure 8 features frames from a Hodson-Nagib film. At $Re_d = 90$ the wake, 111 diameters downstream from the rod, has decayed considerably to u'/U_e of the order of 0.02 to 0.03. The condition of a regular formation of Karman vortex street at approximately 40 Hz was chosen so that the contrast caused by a sudden additional disturbance would be readily perceptible. The sudden disturbance was caused by a single water drop falling on the surface of the water half a channel height above the rod. The effect of the disturbance consists primarily of a sudden change in the phase rather than in the amplitude of the oscillatory wake; the phase change is marked by the letter P in figure 8. We can follow it as it progresses toward the flat face of the rectangular cylinder at the dark vertical line on the left side of the frames. The heads of the oscillating pair of vortices begin to be affected at $t = 0.24$ sec. The evidently forceful ejection of a single horseshoe vortex at $t = 0.44$ sec and further strong vorticity interactions leading to two smaller horseshoe vortices at $t = 0.55$ sec were not previously observed and are initially surprising. They testify to the strength of possible vortical interactions when distributed vorticity is allowed to concentrate locally through instability rollups. The wall gradients associated with such unsteady developments especially in the last two frames of figure 8 are bound to produce high heat transfer rates. Yet the flow is in no sense turbulent. This is regular laminar behavior except for the sudden phase change. The phase change alters the ongoing interactions, which follow the Biot-Savart law. We note that a film was necessary to capture effects due to free-stream disturbances. There are few such films. By focusing first on large disturbances due to steady wall deformations new effects could be captured rather easily because of the fixity of the disturbance. There is reason to believe that an equally rich atlas of interactions, beyond

those of figures 7 and 8, awaits researchers into large steady and unsteady free-stream disturbances.

ROLE OF LOCAL SEPARATIONS

This is an opportune occasion to reinforce the earlier statements concerning local separation as an important effect of large disturbances, steady or unsteady. Obviously the formation of separation pockets cannot be linearized. We have seen local separation play important roles in roughness cases (in fact, practically in all roughness phenomena) and in horseshoe vortex formation at three-dimensional obstacles as well as at blunt leading edges. We should add quasi-two-dimensional local separations at locations of rapid changes of curvature, often called leading-edge bubbles or laminar bubbles even though the closure of the bubble is generally turbulent. The effective mechanism here is inflectional instability. Thin blades and airfoils invariably have separation bubbles. In some cases they are most efficient in making the boundary layer turbulent and thus preventing stall losses in turbomachinery, pumps, and fans.

Even for carefully designed blades, free-stream disturbances with larger velocity components perpendicular to the leading edge, steady or unsteady, may generate separation bubbles locally and temporarily. Part of the research on bypass transition should investigate carefully the local behavior when wakes from upstream are "cutting" across sharp and blunt leading edges of surfaces at various angles so as to systematize and generalize the insights of Hodson and Nagib.

Even when transition is not caused just past the leading edge, large steady and unsteady streamwise vorticity, generated there, affects transition downstream. A significant related observation was made by Kendall (ref. 16) in his figure 5. His turbulence-producing grid was made of slender vertical rods placed in the settling chamber some meters upstream of the measuring station above a horizontal flat plate in the test section. At such distance the intensity u'/U_e in the free stream had decayed to 0.11 percent and was uniform across the span. However, inside the boundary layer the intensity varied regularly from 0.15 to 0.23 percent at spanwise intervals set by the 3.2-mm-diameter rods in the settling chamber. Kendall found the horizontal component u' to be out of phase below and above the plate. Somehow, the u' and w' fluctuations in the rod wakes, antisymmetric in the z direction, were converted into motions antisymmetric in the y direction, perhaps at the leading edge or through vorticity stretching by the 9:1 contraction. How the resulting antisymmetric motion of the stagnation point on the 6:0.5 elliptic nose of the plate was related to the spanwise nonuniformity is not clear. We also know that in very low-disturbance environments significant streamwise vorticity somehow forms in boundary layers (ref. 17) and accelerates the Görtler and crossflow primary instabilities and the secondary instabilities initiated by TS waves. The cause must be sought in the imperfect geometry of the leading edge or in its interaction with free-stream disturbances. Any nick in the leading edge creates a pair of streamwise vortices, and possibly a bypass transition.

In two-dimensional bubbles the rolled-up vorticity of the separated shear layer serves as a rapid turbulizer. If the leading edge is swept or otherwise moves at a skew angle with respect to the local stream, the bubble acquires a throughflow velocity component along its axis. Such formations may grow into

concentrated vortices; if they are cast off the solid surface, they represent strong and dynamic large disturbances that can spoil flows downstream.

FREE-STREAM TURBULENCE AND TRANSITION

Let us now return to effects of free-stream disturbances on transition on undeformed bodies, this time on an ogive-cylinder in an axisymmetric wind tunnel as shown on top of figure 9, borrowed from an unpublished study (ref. 18) of D. Arnal and J.C. Juillen of ONERA, Toulouse. Two free-stream conditions are shown, as indicated by the streamwise x variation of u'/U_e, one with a turbulence-producing grid (grille) and the other without the grid (sans grille). The first lesson from this comparison is that anytime we study effects of free-stream turbulence we must monitor the variation in its intensity and spectra throughout the test section. The intensity of the grid turbulence decreased by more than a factor of 2.5 along the body, while the intensity of the old turbulence from the settling chamber upstream of the contraction increased somewhat.

This latter lack of decay was never explained satisfactorily. In the experience of the author and his colleagues, such a behavior means the probable presence of some slow mean gradients or a swirl with production of new turbulence. Neither of the fields behaves like the idealized isotropic turbulence. Note that neither intensity in these experiments represents really large disturbances. Turbulence of high intensity is invariably spatially nonhomogeneous, and its careful mapping would disclose mean lateral and streamwise gradients in intensity. Quotations of grid-produced turbulence with intensity Tu = $u'/U_e > 0.04$ seldom mention that such fields also exhibit mean velocity gradients when measured along continuous traverses. As we have discussed, such mean gradients modify the boundary-layer amplifiers along their paths. Obviously there is no single Tu number that can characterize the turbulent field as a guide to the onset of transition. No wonder that earlier in this symposium, Ray Gaugler reported failure in predicting transition with all techniques and correlations in the cases of large disturbances he had analyzed. There are too many parameters and subtle nonlinearitites (many not even recorded) to make possible any kind of a credible statistical base for such prediction codes to be trustworthy.

The ONERA study at small-to-medium Tu levels illustrates the dilemmas that we often face as we make more measurements: x_{tr} in the absence of the grid was at 0.9 m, which is upstream of the x_{tr} of 1.05 m achieved in the presence of the grid at much higher Tu. These are measurements by professionals that cannot be dismissed as if they were a beginner's masters thesis. Evidently additional factors, more important than u' levels, must be lurking in the experiments. One such factor could be the spectral distribution of the external disturbances conveyed in the insets of figure 9. The authors confirm that the grid actually suppressed the low-frequency end of the spectrum. Could low-frequency fluctuation of higher amplitude more effectively induce TS waves at higher frequencies (between 400 and 550 Hz) in this flow at 29 m/s? This is not altogether out of the question; one important receptivity path (ref. 19) is through unsteady pressure gradients impressed on the inner boundary layer near and past Re_{cr}. We shall return to this issue in connection with figure 10. Another possibility is that the large disturbances caused by the grid rods planted directly into the wall of the tunnel caused a considerably thicker turbulent boundary layer. The growth of the displacement thickness on the wall must have accelerated the flow somewhat and made the boundary layer

on the body more stable than in the absence of the grid. The authors doubt that this effort was significant, but the measurements of $U_e/U_{e,ref}$ in the upper part of figure 9 were not made near the body. Furthermore, Arnal and Juillen's own figure 42 shows that the displacement thickness of the boundary layer grew about 10 percent faster without the grid, indicating a slightly more destabilizing pressure gradient. We are left with speculations. However, that is a frequent predicament of experimenters in transition, when they make more than one experiment, especially when these are separated by unrelated experiments on the different instruments. It is a very useful lesson for researchers embarking upon the much more demanding task of developing understanding of the effects of large disturbances on the multifaceted phenomena of transition.

Unsteady Disturbances in Laminar Boundary Layers and Receptivity

Figure 10 compares hot-wire traces $u(t)$ at five heights y/θ in the boundary layer as the disturbances inside the layer in the presence of the grid develop with x, where θ is the local momentum thickness at each x. (For approximate estimates we recall that in a Blasius layer $\delta \sim 2.9\delta^* \sim 2.9 \times 2.59\,\theta$.) The first station ($x = 3.7$ cm) is located in the accelerated boundary layer on the nose of the body. Since the time scales in all of the traces are the same, the external high-frequency content (see sample external spectrum in the inset of fig. 9) appears at all the levels of the layer. At the next station, $x = 36$ cm, 10 times as far from the nose, the high frequency has been filtered out or dissipated near the wall. Incidentally, Re_{min} should occur near $x = 15$ cm. The boundary layer on the front of the body is effectively buffeted by the free stream. Upstream of Re_{min} the transport processes across the boundary layer must remain largely laminar (i.e., molecular); the vorticity convected into the parabolic layer and the pressure field of the vorticity remaining outside the layer make it unsteady (i.e., buffet it); see top of figure 14. The small-scale velocity fluctuations carried with the ingested vorticity are effectively damped near the wall. This is evidence against the receptivity path whereby direct free-stream vorticity ingested into the spreading layer would be converted into vertical TS waves. Vorticity entering the layer downstream of Re_{cr} and the vorticity induced by pressure fluctuations across the streamlines remain as possible active agents of receptivity (ref. 19); see top of figure 14.

The small wiggles on the two traces nearest to the wall at x of 66 and 85 cm are in fact the signatures of TS wave packets growing away from the wall. Additional spectral evidence suggests that these TS wave packets keep growing and that after secondary instabilities near $x = 95$ cm and final instabilities near $x = 100$ cm, turbulent intermittency sets in. The important finding is that TS waves first appear near the wall, after all frequencies in the TS range seem to have been filtered out or dissipated upstream. These findings are consistent with the more recent results of Kendall (ref. 16). However, the u' information tells us little about damping of ingested, nearly streamwise vorticity. Such vorticity would produce a zero signal if strictly aligned in the x direction. Since it weaves along its way, all such unsteadiness would be sensed as low-frequency u' signals by the hot wire oriented in the z direction. The low frequencies in the inner y regions at the last two stations are probably partly of this character. However, velocity fields induced by vorticity convected outside the boundary layer should also contribute primarily at lower frequencies: only larger scale formations can influence regions at greater distances (top of fig. 14). Measurements of space-time correlations at two or three points are needed to sort out the complicated

forcing and response fields. Receptivity to free-stream turbulence appears to be very subtle indeed; see Kendall (ref. 16) for additional factual information on the response at a forcing-grid-generated intensity u'/U_e of 0.16 percent.

In the relatively low-intensity experiments of figures 9 and 10, receptivity appears to begin as a linear process seeding linearizable TS wave packets that cumulate and grow to nonlinear levels and lead to higher instabilities. At higher intensities the nonlinear effects described in the section Broad Classification of Large Disturbances should be expected. Important modifications of the oncoming vorticity fields can be anticipated at a sharp leading edge but may be difficult to model.

When a turbulent field approaches a blunt body, the potential field induced by the blunt shape distorts the turbulent field substantially and non-isotropically. It is the distorted field that ultimately interacts with the boundary layer. A serviceable account of the transformed field is obtainable through the so-called "rapid distortion theory" (ref. 20). If applied to ω_z vorticity in figure 6, the theory would indicate that such vorticity is stretched and amplified algebraically as it is convected toward the blunt body. The vorticity lines also deform into a horseshoe shape as they approach the body. Once they penetrate deeply enough into the boundary layer the stretching is counteracted by viscosity and the associated disturbances damp, at least at the linearized level of stability analysis.

A very useful outline of the many phenomena discovered in fields where different turbulent or vortical flows convect into or impinge upon a body is in the recent survey of Bushnell (ref. 21).

LAMINAR BOUNDARY LAYERS BUFFETED BY INTENSE TURBULENCE

What happens in the boundary layers upstream of Re_{min}? As noted in connection with figure 10, there may be a great deal of activity near the wall, much of it dissipated at the low Reynolds number. The dominant mode of transfer remains molecular. However, the ONERA disturbance levels were relatively low. When the stream contains large disturbances, we run into the problem of defining and describing the dominant characteristics of such flows, as discussed earlier in the section on classification. There are many isolated reports on transition, heat transfer, drag, and other overall "outputs" with inadequately defined conditions. Such usually ad hoc tests are often contradictory and leave a great deal of uncertainty in their wake, primarily because the results are not documented in terms of mechanisms or detailed flow behavior. A valid criticism by Dyban, Epik, and Suprun (ref. 22) states, "The observed augmentation of transfer processes (in a layer that remains laminar) is 10 to 80 percent (four quoted references) . . . very little was published on the mechanism of the interaction . . ." The results of Dyban and co-workers, a small sample of which is summarized in figures 11 and 12, deserve attention and an attempt at duplication to see whether turbulent buffeting would act the same way in the United States as it did in Kiev.

Such a suggestion is much more than a joke and deserves clarification. Contradictory and unconfirmed overall "outputs" (such as mean position of transition, average heat transfer over larger areas, drag, etc., labeled "macroscopic measurements" by Lester Lees) were recognized as a major block in the progress of transition research in 1970 by the U.S. Transition Study Group (currently an informal group, chaired by Eli Reshotko). To remedy such

uncertainties and to avoid miscues for further research, USTSG adopted (among others) guideline 4 (ref. 23): "Whenever possible, tests should involve more than one facility; tests should have ranges of overlapping parameters, and whenever possible, experiments should have redundancy in transition measurements." In my function here as a preacher, I would paraphrase Lees: "Go microscopic research (seek detailed mechanisms), young man or woman!" and add, "In transition research, duplicating key measurements is not a Sin, it's a Virtue." In 1977, I broadened (ref. 24) guideline 4 to computer research, whereby by "facility" we understand a theoretical model, however simplified, with its computer program. A case in point is the recent public confusion (ref. 25) concerning supersonic instability, when contradictory numerical results went to print without insistence on rigorous prepublication comparison of the two codes.

Most careful researchers believe that "higher values of free-stream turbulence can be achieved only with increasing inhomogeneous distributions of dynamic head and turbulence across the test section" (ref. 26). On the other hand the Kiev group claims that it is possible to achieve "virtually complete uniformity of the spatial distribution of fluctuating and average velocities at the test section inlet" by the use of high-solidity grids – provided they are placed just ahead of the converging section of the wind tunnel. Hassan Nagib, who was originally skeptical, tells me now that the scheme has possibilities because the immediate acceleration through the contraction may prevent the "anomalous" behavior of high-solidity inserts. (The pressure drop across high-solidity devices is high; in fact they produce multiple jets which have a tendency toward random coalescence, "anomalous" nonhomogeneity, low-frequency intermittency, and spurious intensity growth. This is discussed on page 33 of reference 27, a mechanism oriented text indispensable to researchers into the effects of turbulence.) The Kiev group has approached practical high-turbulence research more systematically than others, and their published results exhibit unexpected consistency.

The abstract in figure 11 describes adequately the six figures in the paper. The graphs in figure 11 convey the development of the mean profiles, including their substantial thickening as compared with the Blasius profile, labeled I. The measurements at the Reynolds numbers noted in figure 11 were achieved with hot-wire anemometers at a free-stream speed of 0.88 m/s at distances x of 105 and 340 mm from the nose of the flat plate sketched in the margin of figure 12. Figure 11 suggests a considerable increase in the slope at the wall at intensities of 8 to 10 percent. In figure 1 of another paper in English, Dyban and Epik (ref. 28) display measured u', v', and w' distribution through evidently the same boundary layer at $Re_x = 20\ 000$. They infer that they also measured the Reynold stress $\overline{uv}$ from Blasius $\eta = 1.5$ outward. Extrapolation to the wall yields an increment of some 45 percent over the laminar value for $Tu \sim 9$ percent in figure 7 of reference 28; see also the three circles (i.e., the three data points in the curve for skin friction C_f in the top graph of our fig. 12). As marked in the margin of that graph, the authors assure us that in the buffeted layers, which they call pseudolaminar, the displacement thickness remains "virtually constant." The shape factor H then decreases from the Blasius value to the 1.9 plateau because the skin friction and momentum thickness (which they denote by δ^{**}) grow as Tu is increased to 14 percent. (In ref. 27, they force-fit the rise in C_f and the Nusselt number Nu with Tu by a second-degree polynomial in Tu and go on to link it with eddy viscosity and other prediction formulas. The quadratic fit would yield a factor of 1.98 for $C_f/C_{f,0}$, which contradicts the top graph

in our figure 12. They arbitrarily limit the predictions to $Tu \sim 14$ percent, the beginning of the plateau in that graph.)

The lower graph in figure 12 displays the intensity distributions u' through the boundary layer as a function of free-stream forcing u_∞. They focus on the position of the maximum u'_{max} in the boundary layer as a measure of the "penetration of the fluctuations" referred to in the abstract and in their figure 4; they feel it is independent of Reynolds number. However, very pronounced u'_{max} greater than 8 to 10 u_∞ in laminar layers was observed in the 1950's by A. Favre (personal communication) and P. Klebanoff for low u_∞; see top of figure 14. This effect, described and referred to as the Klebanoff mode of fluctuations by Kendall (ref. 16), has been explained as a "low-frequency breathing effect"; as the quasi-static Blasius profile shifts with slow thickening and thinning of the layer, the maximum Δu felt by a hot wire at a fixed height is near $\delta/2$. The breathing effect is in no sense dynamic. The dominant contributions to the signal u'_{max} at $\eta = 2.5$ for $u_\infty = 9.69°$ in the lower part of figure 12 are well below 150 Hz; therefore the slow thickening-thinning effect probably has nonnegligible influence on the formation of the u' peak inside the layer even at this high forcing intensity. Some of the authors' interpretations should therefore be accepted temporarily with much caution. Note also that the reader is given no $u'(x)$ decay curve such as was provided by Arnal and Juillen in the lower part of figure 9.

Dyban and Epik (ref. 28) infer that at $Re_x = 60\ 000$ the "initial" boundary layer is turbulent. That this would be so for their lowest Tu value of 0.31 percent would be surprising; nevertheless this is as close as they come to the concept of Re_{min}. (Nor is there any discussion of laminar-turbulent intermittency, which would be difficult to identify without a thermal tracer.) They call the initially turbulent layers disturbed by external Tu pseudo-turbulent boundary layers and refer perturbed c^f to the turbulent wall

friction at their lowest u_∞. They measure u', v', w', $\overline{uv}$, c^f, and Nu and interpret the results in terms of a mixing length for prediction purposes. The prediction range once again has to be limited to $Tu < 14$ percent. Their figure 3 for $u_\infty = 6.85$ percent at $Re_x = 400\ 000$ is particularly interesting. First, u'_∞, v'_∞, and w'_∞ are within 6 percent of each other; this achievement of near isotropy at these high turbulence levels lends credibility to their effort. Second, v' has no maximum within the layer, rising monotonically outward to v'_∞; u' and v' on the other hand rise monotonically toward the wall, presumably to maximums at the edge of the sublayer, which remains instrumentally unresolved. Through this account of some of the work of the Kiev group, in the role of an objective reporter I am calling the attention of the researchers starting along this road to this essentially unknown existing systematic information. In my role as a preacher, I am adding the address: Prof. Evgenii Pavlovich Dyban and Dr. Eleanora Yakovlieva Epik, Inst. Techn. Thermophysics, Ukrainian Academy of Sciences, 2a Zhelabova Ul., 252057 Kiev, USSR, in case detente should break out some spring.

LOOKING BACK

Now that we have examined the concepts of Re_{min} and bypasses, identified some of them, classified large disturbances (with special stress on the large mean and quasi-steady distortions of the wall or the free stream as creating bypass amplifiers), acquired some "feel" for their effects via graphic examples of such distortions from protuberances, horseshoe vortices, local separations, and steady and unsteady wake distortions of the stream to more

statistically regular turbulence, large, medium, and small, let us look at a few overview figures. Figures 13 and 14 provide the overall setting for our problem and should make us appreciate why we are up against an especially difficult one. To understand nonunique solutions of nonlinear partial differential equations in four independent variables with very small coefficients of the highest derivatives (viscosity and heat conductivity) is a tall order indeed. Fluid dynamics of generalized Navier-Stokes equations requires us to make sense out of a concatenation of interlaced singular perturbations with multiplicities of solutions. Instabilities represent rapidly crossed moving bridges between subsets of the multiplicity of solutions reachable from physically ill-defined initial conditions at the entry to our open fluid systems. As velocity or x, and hence Re, increase, the effective degrees of freedom increase and so does the large sensitivity to initial conditions. The solutions evolve toward "turbulence."

Actually, it is difficult to define turbulent solutions of the Navier-Stokes equations. As fluid dynamicists we require the presence of the four syndromes in figure 13 to identify turbulent behavior. Syndrome 1, which is used to define "strange attractors," is insufficient for our needs. An examination question: where does a laminar boundary layer buffeted by high external turbulence fit here, and how can we distinguish it empirically from a turbulent boundary layer? The concept is important for design. How can we study it experimentally? In the real world, all laminar boundary layers are buffeted by decaying free-stream turbulence (which remains turbulent as long as there are nonlinear interactions, as intermittent in time and space as these may be). We have little difficulty with that idea as long as transition is downstream of Re_{cr}. The real difficulty faces us near Re_{min}. Of all the syndromes, only syndrome 3, diffusion far in excess of molecular mixing, can guide us. Some of the speculations I offered earlier were based on the assumption that little true turbulent mixing could go on at the scale of local δ below Re_{min}. However, we can imagine a large unsteady turbulent event passing by, say 40δ in length. The temporarily thickened Re_θ may well exceed $Re_{\theta,min}$. Turbulent patches can form in ducts at $Re \approx 1000$, but they decay unless Re exceeds 1500. In response to intermittent large disturbances, intermittent decaying turbulent spots could exist upstream of nominal Re_{min}. If so, the time-average heat or mass transfer would rise much more gradually through the nominal location of Re_{min}. The 1.55 asymptote of the upper graph for skin friction in figure 10 of Dyban et al. (ref. 22) is rather reassuring. The growth curve through Re_{min} may "smear" the contrast in transport behavior, but there should be a practically important upper bound for that transfer rate.

Figure 14 summarizes the processes discussed in connection with figures 9 to 12 as they were driven by free-stream turbulence. A few extra comments are in order: (1) In connection with the ONERA cases we noted that the turbulent vorticity ingested near the leading edge had its finer scales dissipated by viscous wall action; the filtering was so effective that, when the TS waves with wavelengths of 8δ and longer finally grew (fig. 8), they represented higher frequencies and may have been induced across the boundary layer by external turbulent vorticity, as indicated in figure 14 by the label "at distance." (2) TS (or equivalent) waves exist and are induced upstream of the TS Re_{cr}. Forcing motion in linearized system equations induces homogeneous solutions (i.e., decaying or growing eigenfunctions) by the requirement that all boundary conditions be satisfied. Upstream of Re_{cr}, the induced TS response decays shortly after its birth.

The lower sketch in figure 14 adds the effects of an isolated three-dimensional roughness. These we discussed in considerable detail in connection with figures 2 and 5. Finally we noted that in the known systems $Re_{min} <$ Re_{cr}, except for the zero-pressure-gradient case, where $Re_{min} \sim Re_{cr}$.

LOOKING FORWARD

The 1984 view of paths to wall turbulence in mildly disturbed environments (fig. 15) can help to organize our thoughts on research into the effects of large disturbances. We need to start with a conceptual framework to project best-bet experiments linked in a systematic way.

Let us review the ingredients along the paths to turbulence and consider how their role is changed because of the higher disturbances. The standard primary linear instabilities (TS, Görtler, and crossflow half-way up in the figure) still can amplify the initially much larger vorticity disturbances (e.g., the visualized nonlinear TS wave packets for $Tu \sim 3.6$ percent in figure 9 of E.M. Gates (ref. 29)). We can expect strong effects of the centrifugal instability (of the Görtler type) in the concave regions of turbine blades, both before and after (!) transition; see Bradshaw (ref. 30) (an important reference for heat transfer estimators).

However, the major upstream movements of transition should come from the quasi-steady, larger scale three-dimensional shear layers carried with the flow, which modify our standard base flows (i.e., our amplifier systems). Because the probably spotty and intermittent regions of largest disturbance bring to the vicinity of the wall three-dimensional vorticity components stronger than those that effect the swift secondary instabilities in the middle of figure 15, we can say – with not much exaggeration – that we essentially begin with a broader class of discretely sprinkled, moving, fast secondary instabilities. (In bypass transitions I expect to see the number in the sequence of instabilities leading to turbulence cut at least by one, in comparison with the standard paths of fig. 15.) But the total number of possible instability paths may be larger. As discussed in the section on classification and illustrated herein (e.g., fig. 8), the larger scales are likely to generate instantaneous three-dimensional profiles (possibly with local separation) subject to inviscid instabilities fast enough to lead all the way to turbulence during the lifetime of these boundary-layer distortions.

Such detailed unsteady behavior is very difficult to document experimentally: instrumental space-time resolution and adequate probe access and traversing with minimal flow interference are major problems. In practical flow configurations, unless we make a heroic effort, the disturbances are likely to be characterized by only one or two averaged parameters and the measured boundary-layer profiles, and "macroscopic" outputs at the wall (even when measured as functions of x) are also severely averaged. Such information is therefore unlikely to lead to better understanding of the particular mechanisms involved in the increased heat transfer. Nor will the smeared information lead to inspired ideas for improvements in design: it does not provide enough linkage between true causes and the measured, averaged output.

Such information will also aid little in modeling and computational code development, for much the same reasons. As I mentioned earlier I am quite pessimistic about Navier-Stokes codes being able to resolve in time and space the clearly important unsteady flows near leading edges such as the sample in

frames 4 to 6 of figure 8 or the transition in the old bypass of the blunt-body paradox, at least for a few decades. So, codes must use grosser modeling. More primitive modeling seldom leads to improved physical insight. For instance, in an earlier talk we heard about the relative success of the Chorin vortex simulation of the flow downstream of a backward-facing step, aimed at one of the simpler cases of combustion. The important simplifications in the model were two-dimensionality of the vortex filaments and neglect of viscosity - for the good physical reasons that the separated shear layers are subject to a quasi-two-dimensional inviscid instability, whether the layer is laminar or turbulent. At least two aspects will have to be added to the model: the presence of the wall below the shear layer and at the termination of the chamber. Actually, the physical effects that those features introduce are three-dimensionality of the vorticity and compressibility. The reason for the first is that the shear layer is three-dimensionally unstable as it approaches the reattachment line on the wall below the layer. From my years at Martin-Marietta Co., I recall an experimental paper, then classified, showing spanwise maximum-minimum variation of heat transfer rates in a ratio of 3 to 1 along the mean reattachment line. The maximums were dangerous for the controls on our maneuverable reentry vehicle, the SV5, and would be undesirable should they occur in the presence of combustion. George Inger refers to it in his linear analysis (ref. 31) of the instability; Anatal Roshko has been interested in this three-dimensionalization of reattachment flows for over two decades and recently has obtained some interesting results (unpublished) that could inspire better local modeling. Adding three-dimensionality of the individual vortices to Chorin's model amounts to more than a slight generalization. Mostly because of the vorticity source term $\vec{\omega} \cdot \text{grad}(\vec{v})$ mentioned in the section on classification, the task is harder than Chorin's developments to the present form of the technique.

FINAL INTERLUDE ON FREE-STREAM DISTURBANCES

The example of the termination of the combustion chamber was chosen mostly to emphasize that free-stream disturbances tend to be overidentified with turbulence (i.e., vorticity and its induced velocity field). It is well known that, when shear flows impinge on a rigid surface, pressure feedback is directed upstream and strongly influences the instability of the separated shear layer and any associated combustion. Incompressibility allows only instantaneous pressure feedback, essentially the near-field acoustic behavior; sound (essentially the far-field behavior) is not allowed and with it many potentially dangerous acoustic resonances common to shear layers separating cleanly from a solid surface. Receptivity to unsteady pressure gradients is one or two orders of magnitude higher at separation lines than it is in unseparated shear layers. (This is the reason why instabilities at isolated three-dimensional excrescences such as seen in fig. 3 are easily pumped up acoustically - forced at distances across streamlines. For x_k past Re_{cr}, transition can thereby be moved substantially upstream.) Realistic prediction codes and diagnostics of free-stream disturbances should allow for such feedback and resonant coupling.

The Chorin model was used only to illustrate the fact that simplified codes quite generally will not be able to simulate satisfactorily this or that mechanism of importance in our transition phenomena. Codes therefore will not be generally able to guide the experiments.

Returning to large free-stream disturbances, the preceding discussion indicates that their theoretical and experimental definition must include unsteady pressure gradients: hydrodynamic (near-field acoustic) and acoustic (far field). The unsteady input disturbances (A.C.) in figure 15 for linearizable amplitudes include entropy disturbances (i.e., density-temperature nonhomogenities (with negligible Δp) convected with the fluid). Such moving entropy nonhomogenities can induce TS waves at supersonic speeds, but the strength of the effect has not been investigated. It has been assumed to be of secondary importance. This is unlikely to be warranted when cooling elements or combustion are present. On the other hand, the unsteady pressure field (sound) generated by turbulent boundary layers on the side walls is known to be so strong and effective at supersonic speeds that it spoils most studies of transition in wind tunnels from Mach 1.5 to 6 or 7; the transition modes that would be present in free flight are bypassed and preempted by the sound forcing.

Ideally, to classify a large free-stream disturbance, we would like to distinguish its steady or moving coherent features from the more homogeneous turbulent background (such as explored by Dyban's Kiev group (refs. 22 and 28)). The first task would then be to identify the stronger, more regular features such as moving shock waves, quasi-two-dimensional wakes from upstream obstacles, free concentrated vortices, and swirl. This requires good understanding of the flow prehistory; such knowledge would then guide subtle diagnostics with two probes, one of which must be traversing within the inlet plane.

The same instrumentation can provide estimates of near-field pressures and far-field acoustic fields. The coherent velocity amplitude of each spectral peak correlated across the inlet plane or test section yields the acoustic field. For nearly plane far-field waves the pressure fluctuation is equal to ρa times the normal velocity fluctuations, where ρ and a are the local mean density and speed of sound, respectively. Few researchers recognize to what extent the low-frequency end of the velocity spectrum measured at the inlet of their test section is actually driven by near-field pressure fluctuations (also called pseudosound). From experience I would guess for instance that more than 50 percent of the very low-frequency contribution to the measured u'/U_e "sans grille" in the inset of figure 9 comes from such pressure fluctuations, which are given very nearly by $\rho U_e u'$. This is a linearized Bernoulli relation for u' fields correlated across the inlet plane. Since the low frequencies correspond to acoustic wavelengths that are far longer than the test section, the sources of the near-field pressure (usually random-like and broadband) can be quite distant. Some of these disturbances come from downstream, as, for example, the low-frequency part of the pressure feedback mentioned earlier (refs. 32 and 33). The role of relatively large, low-frequency pressure fluctuations in the transition process is not clear, but there is some indirect evidence that they contribute to receptivity, especially in the presence of small distributed roughness. They and the acoustic disturbances should be added to the top of figure 14 as additional receptivity paths. Their temporal irregularity evidently modulates the time development of whatever instabilities do arise, forcing random characteristics upon the primary and higher modes long before there is turbulence of the shear layer itself.

Ideally, after identifying the contributions from swirl, shock waves, wakes, and free vortices as well as from the acoustic and near-field fluctuations, we should be able to subtract them in the square from total fluctuation signals and to obtain the residual free-stream turbulences, provided that there

were no significant entropy fluctuations. If there is upstream cooling or combustion, additional probes for measurements of temperature fluctuations will be needed. Should the residual turbulent and entropy fluctuations turn out to be quite uniformly distributed over the inlet section, that would be an indication of the consistency of the decomposition process. When we include spectral and correlation characteristics relevant to the transition process, the number of free-stream parameters will generally exceed 5 and could run past 10 for more complex flows. Also there will be nonnegligible uncertainty concerning each parameter.

It should be fairly clear that after such ideally effective measurements we still would have difficulties relating the input parameters to the output measurements, even if we (still more ideally) could vary the free-stream parameters rather freely in our experiments. We need only to reflect on the lessons from the orders-of-magnitude simpler example of figure 9, where the low-Tu conditions induced an earlier transition. (A third condition with stronger grid-turbulence did not resolve the puzzle.)

REPRISE

From the preceding exercise it appears that a frontal approach to practical flow configurations is likely to run into severe difficulties in defining experimentally the requisite environmental parameters on one hand and in interpreting meaningfully the "output measurements" on the other. Yet, as in all research directed at specific applications, there will be strong pressures to look at the "real thing." A preacher is expected to evoke the path to righteousness, even when he is ignorant of "practical life." So perhaps I may be permitted to give my insufficiently informed views. My experimental bias would be to strive first to establish a qualitative framework of understanding by clarifying individually as many important mechanisms and interaction patterns as can be anticipated. As we have seen, key elements in the interactions are likely to be isolated wakes and vortices coming from different angles toward the leading edges (blunt, slender, and sharp). For strong disturbances the main action of interest should take place from just upstream of the leading edge to past Re_{min}, perhaps to Re_{cr}. Access, transversing of the velocity and thermal fields, and visibility (if possible) in these regions are important. Broadly speaking we could proceed in the spirit of figures 5 and 6 of Hodson and Nagib (ref. 14) to generalize their insight systematically to as many separate geometrical variants as the ingredients in practical configurations would suggest. Each conceptual experiment would have a small number of controlling parameters so that connections between cause and effect could be made with some confidence.

Such simplification and conceptualization is more likely to lead to improvements in codes and design: it more frequently inspires "cures" should particularly detrimental conditions be identified (such as local separation). It was such a simplified wind tunnel test that identified and developed a cure for the dangerous bypass on sweptback aircraft (turbulence contamination from the fuselage juncture to the attachment layer on the leading edge of the wing (ref. 34) – see the section Flows with Known $Re_{\theta,min}$ and Re_{cr}). "Practical" flight tests had failed to improve the poor performance. We note that the experiments of Dyban et al. (refs. 22 and 28) are also simplified in that they strove to make the large turbulence homogeneous and nearly isotropic, so that the relevant parameters were reduced to Tu and the velocity spectrum. (In any recheck of their results attention to the role of the leading edge would

be desirable: measurements just upstream and just downstream, with at least one variant from their sharp edge, to clarify the restructuring of the field and possible local separation in the presence of the large fluctuation normal to the edge.)

From the simpler experiments we could proceed to compound problems, such as combination of wakes approaching bodies with increased free-stream turbulence (homogeneous Tu outside the wakes) to assess the effects of "superposition." The compounding would of course aim at approximating progressively the suspected structure of the environment in key practical configurations. The problem of the "scrubbing" heat transfer at junctures and hubs of blades, where boundary layers (with local separation) on two walls interact, can be approached in a similar conceptual manner. Any time there is a mean velocity component along the leading edge of a blade, a counterpart of the strong contamination bypass encountered on sweptback wings (ref. 34) becomes a potential danger. (Away from the attachment line lateral contamination influences a substantially smaller domain, limited by the spreading angle of the order of 10° from the local potential streamline at the edge of the boundary layer.)

As we commented in connection with the visualization figures, to start with low Reynolds numbers has many experimental and conceptual advantages, in particular space-time resolution and visibility. In experiments at the prototype Reynolds numbers with large disturbances, the transition phenomena that we seek to understand will occur at low Reynolds numbers based on the distance from the leading edge, anyway, but on spatial and temporal scales that are much harder to resolve. I think I am beginning to repeat myself and the obvious as well. In fact, many of the attitudes I am preaching are evident in the papers on NASA Lewis research in progress, in particular those of Jim VanFossen and Barbara Brigham. So I can quit preaching with the sense that the flock knows the way to the Promised Land. Nevertheless, let me remind you in parting to heed the wisdom of the four guidelines for transition research on page 345 of Eli Resotko's review (ref. 23).

REFERENCES

1. Peterson, J.B.; and Horton, E.A.: An Investigation of the Effects of a Highly Favorable Pressure Gradient on Boundary-Layer Transition as Caused by Various Types of Roughnessess on a 10-Foot-Diameter Hemisphere at Subsonic Speeds. NASA Memo 2-8-59L, 1959.

2. Murphy, J.D.; and Rubesin M.W.: A Re-Evaluation of Heat Transfer Data Obtained in Flight Tests of Heat-Sink Shielded Re-Entry Vehicles, J. Spacecraft and Rockets, vol. 3, 1966, p. 53.

3. Morkovin, M.W.: Critical Evaluation of Transition from Laminar to Turbulent Shear Layers with Emphasis on Hypersonically Traveling Bodies. AFFDL TR-68-149, 1969.

4. Schübauer, G.B.; and Klebanoff P.S.: Contributions on the Mechanics of Boundary Layer Transition. NACA Tech. Rept. 1289, 1956.

5. Klebanoff, P.S.; Schubauer, G.B.; and Tidstrom, K.D.: Measurements of the Effect of Two-Dimensional and Three-Dimensional Roughness Elements on Boundary-Layer Transition, J. Aero. Sci., vol. 22, 1955, pp. 803-804.

6. Wygnanski, I.J.; and Champagne F.H.: On Transition in a Pipe. Part 1. The Origin of Puffs and Slugs and the Flow in a Turbulent Slug, J. Fluid Mech., vol. 59, No. 2, 1973, pp. 281-335.

7. Carlson, D.R.; Widnall, S.E.; and Peeters, M.T.: A Flow-Visualization Study of Transition in Place Poiseville Flow, J. Fluid. Mech., vol. 121, 1982, pp. 487-505.

8. Poll, P.J.A.: Transition in the Infinite Swept Attachment Line Boundary Layer, Aero. Quart, vol. 30, 1979, pp. 607-629.

9. Hall, P.; Malik, M.R.; and Poll, D.I.A.: On the Stability of an Infinite Swept Attachment Line Boundary Layer, Proc. Roy. Soc. London A, vol. 395, 1984, pp. 229-245.

10. Preston, J.H.: The Minimum Reynolds Number for a Turbulent Boundary Layer and the Selection of a Transition Device, J. Fluid. Mech., vol. 3, 1958, pp. 373-384. (To be modified in accordance with p. 1418 of D. Coles in Phys. Fluids, vol. 7, pp. 1403-1423.)

11. Herbert, Th.: Secondary Instability of Shear Flow. Nonlinear Effects in Hydrodynamic Stability, Sections 7 and 6 in the Special Course on Stability and Transition of Laminar FLow. AGARD Rept. 709, NATO, Paris, 1984. (Available through National Technical Infomation Services, 5285 Port Royal Road, Springfield, VA 22161.)

12. Gregory, N.; and Walker, W.S.: The Effects of Transition of Isolated Surface Excrescences in the Boundary Layer. British ARC, Res. Memo. 2779, 1956.

13. Norman, R.S.: On Obstacle Generated Secondary Flows in Laminar Boundary Layers and Transition to Turbulence. Ph.D. Thesis, Ill. Inst. Tech., 1972. (Available from University Microfilms International, 300 N. Zeeb Rd., Ann Arbor, MI 48106.)

14. Hodson, P.R.; and Nagib, H.M.: Longitudinal Vortices Induced in a Stagnation Region by Wakes - Their Incipient Formation and Effects on Heat Transfer from Cylinders. NASA CR-152850, 1975. (Condensed in Progress in Astronautics and Aeronautics, vol. 59, 1977, pp. 66-90.)

15. Morkovin, M.V.: On the Question of Instabilities Upstream of Cylindrical Bodies. NASA CR-3231, 1979.

16. Kendall, J.M.: Experiments on the Generation of Tollmien-Schlichting Waves in a Flat-Plate Boundary Layer by Weak Free-Stream Disturbances. AIAA Paper 84-0111, 1984.

17. Anders, J.B.; and Blackwelder, R.F.: Longitudinal Vortices in a Transitioning Boundary Layer, in Laminar - Turbulent Transition, Eppler, R. and Fasel, H., eds., Springer Verlag, 1980, pp. 110-119.

18. Arnal, D.; and Juillen, J.C.: Experimental Contribution to the Study of Receptivity to Turbulence of a Laminar Boundary Layer (in French). ONERA, CERT, DERA Rpt. 1/5018 DY, 31055 Toulouse, 1978.

19. Nishioka, M.; and Morkovin, M.V.: Boundary-Layer Receptivity to Unsteady Pressure Gradients: Experiments and Overview 1984. (Submitted to J. Fluid Mech.)

20. Townsend, A.A.: The Structure of Turbulent Shear Flow, Cambridge Univ. Press, 1976, pp. 71-88.

21. Bushnell, D.M.: Body-Turbulence Interaction, AIAA Paper 84-1527, 1984. (Presented at 17th Fluid Dynamics and Plasmadynamics Conference, Snowmass, CO, June 1984.)

22. Dyban, Ye.P.; Epik, E.Ya.; and Suprun, T.T.: Characteristics of the Laminar Boundary Layer in the Presence of Elevated Free-Stream Turbulence. Fluid Mechanics - Soviet Research, vol. 5, no. 4, 1976, pp. 30-36.

23. Reshotko, E.: Boundary-Layer Stability and Transition. Annual Reviews of Fluid Mechanics, vol. 8, 1976, pp. 311-350 (especially p. 345), Annual Reviews, Palo Alto, CA, 94306.

24. Morkovin, M.V.: Instability, Transition to Turbulence, and Predictability. Keynote address at AGARD Copenhagen Symposium, May 1977. AGARDograph 236, NATO, 1978. (Available through National Technical Information Services, 5285 Port Royal Road, Springfield, VA, 22161.)

25. Mack, L.M.: Remarks on Disputed Numerical Results in Compressible Boundary-Layer Stability Theory, Phys. Fluids, vol. 27, 1984, pp. 342-347.

26. Kiock, R.; Laskowski, G.; and Hoheisel, H.: The Generation of Higher Levels of Turbulence in the Test Section of the High-Speed Cascade Wind Tunnel at Braunschweig for Simulation of Turbomachinery Conditions (in German). DFVLR-Forschungsbericht, 1982, 54 pages.

27. Loehrke, R.I.; and Nagib, H.M.: Experiments on Management on Free-Stream Turbulence, AGARD Rept. 598, NATO, 1972. (Available through National Technical Information Services, 5285 Port Royal Road, Springfield, VA, 22161, as AGARD Rept. or as AD749891.)

28. Dyban, E.P.; and Epik, E.Ya.: Heat Transfer in a Boundary Layer in a Turbulized Air Flow, Vol. 2, Proceedings Sixth International Heat Transfer Conference, Toronto, Canada, Aug. 1978, pp. 507-512.

29. Gates, E.M.: Observations of Transition on Some Axisymmetric Bodies, Laminar-Turbulent Transition, Eppler, R. and Fasel, H., eds., Springer Verlag, 1980, pp. 351-363.

30. Bradshaw, P.: Effects of Streamline Curvature on Turbulent Flow, AGARDograph 169, AGARD, NATO, 1973. (Available through NTIS.)

31. Inger, G.: Three-Dimensional Heat and Mass Transfer Effects Across High-Speed Reattachment Flows, AIAA J., vol. 15, 1977, pp. 383-389.

32. Wills, J.A.B.: Spurious Pressure Fluctuations in Wind Tunnels. J. Acoust. Soc. A., vol. 43, no. 5, May 1968, pp. 1049-1054.

33. Dimotakis, P.E.; and Brown, G.L.: The Mixing Layer at High Reynolds Number: Large-Structure Dynamics and Entrainment. J. Fluid Mech., vol. 78, 1976, pp. 535-560.

34. Gaster, M.: A Simple Device for Preventing Contamination on Swept Leading Edges, J. Roy. Aero, Soc., vol. 69, 1965, p. 788.

BIBLIOGRAPHY

1. Liebert, C.H.; Gaugler, R.E.; and Gladden, H.J.: Measured and Calculated Wall Temperatures on Air-Cooled Turbine Vanes with Boundary Layer Transition. ASME Paper 83-GT-33, 1983.

2. Dillon, R.E.; Watervliet, N.Y.; and Nagamatsu, H.T.: Heat Transfer Rate for Laminar, Transition, and Turbulent Boundary Layer and Transition Phenomenon on Shock Tube Wall. AIAA Paper 82-0032, Jan. 1982.

3. Liepmann, H.W.; and Nosenchuck, D.M.: Active Control of Laminar-Turbulent Transition. J. Fluid Mech., vol. 118, May 1982, pp. 201-204.

4. Priddy, W.J.; and Bayley, F.J.: Heat Transfer to Turbine Blading. Heat and Mass Transfer in Rotating Machinery, D.E. Metzger and N.H. Afgan, eds., Hemisphere Pub. Co., Washington, 1984, pp. 427-438.

5. Wazzan, A.R.; and Taghavi, H.: The Effect of Heat Transfer of Three-Dimensional Spacial Stability and Transition of Flat-Plate Boundary Layer at Mach 3. Int. J. Heat Mass Transfer, vol. 25, no. 9, Sept. 1982, pp. 1321-1331.

6. Brown, A.; and Martin B.W.: Flow Transition Phenomena and Heat Transfer Over the Pressure Surfaces of Gas Turbine Blades. ASME Paper 81-GT-107, Mar. 1981.

7. Daniels, L.D.; and Browne, W.B.: Calculation of Heat Transfer Rates to Gas Turbine Blades. Int. J. Heat Mass Transfer, vol. 24, no. 5, May 1981, pp. 871-879.

8. Tani, I.: Three-Dimensional Aspects of Boundary Layer Transition. Proc. - Indian Acad. Sci., Eng. Sci., vol. 4, Aug. 1981, pp. 219-235, 237, 238.

9. Abu-Ghannam, B.J.; and Shaw, R.: Natural Transition of Boundary Layers - The Effects of Turbulence, Pressure Gradient and Flow History. J. Mech. Eng. Sci., vol. 22, no. 5, Oct. 1980, pp. 213-228.

10. Martin, B.W.; and Brown, A.: Factors Influencing Heat Transfer to the Pressure Surfaces of Gas Turbine Blades. Int. J. Heat Fluid Flow, vol. 1, no. 3, 1979, pp. 107-114.

11. Bippes, H.: Experimental Study of the Laminar-Turbulent Transition of a Concave Wall in a Parallel Flow. NASA TM-75243, 1978.

12. Cebeci, T.; and Brawshaw, P.: Momentum Transfer in Boundary Layers, Hemisphere, 1977.

13. Forest, A.E.: Engineering Predictions of Transitional Boundary Layers. Laminar-Turbulent Transition. AGARD CP-224, 1977, pp. 22-1 to 22-19.

14. Mack, L.M.: Transition Prediction and Linear Stability Theory. Laminar-Turbulent Transition. AGARD CP-224, 1977, pp. 1-1 to 1-22.

15. Reshotko, E.: Boundary Layer Stability and Transition. Annual Review of Fluid Mechanics, Vol. 8, 1976, pp. 311-350.

16. Bushnell, D.M.; Cary, A.M. Jr.; and Holley, B.B.: Mixing Length in Low Reynolds Number Compressible Turbulent Boundary Layers. AIAA J., vol. 13, no. 8, Aug. 1975, pp. 1119-1121.

17. Kaups, K.: Transition Prediction on Bodies of Revolution. MDC-J6530, Douglas Aircraft Co., 1975. (AD-778045.)

18. Merkli, P.; and Thomann, H.: Transition to Turbulence in Oscillating Pipe Flow. J. Fluid Mech., vol. 68, part 3, Apr. 15, 1975, pp. 567-576.

19. Reshotko, Eli: A Program for Transition Research. AIAA J., vol. 13, no. 3, Mar. 1975, pp. 261-265.

20. Cebeci, T.; and Smith, A.M.O.: Analysis of Turbulent Boundary Layers. Academic Press, 1974.

21. McDonald, H.; and Fish, R.W.: Practical Calculations of Transitional Boundary Layers. Int. J. Heat Mass Transfer, vol. 16, no. 9, Sept. 1973, pp. 1729-1744.

22. Dunham, J.: Predictions of Boundary Layer Transition on Turbomachinery Blades. Boundary Layer Effects in Turbomachines. AGARD AG-164, 1972, pp. 55-71.

23. Hall, D.J.; and Gibbings, J.C.: Influence of Stream Turbulence and Pressure Gradient upon Boundary Layer Transition. J. Mech. Eng. Sci., vol. 14, no. 2, Apr. 1972, pp. 134-146.

24. Kobayashi, Ryoji: A Note on the Stability of a Boundary Layer on a Concave Wall with Suction. J. Fluid Mech., vol. 52, part 2, Mar. 28, 1972, pp. 269-272.

25. Seyb, N.J.: The Role of Boundary Layers in Axial Flow Turbomachines and the Predictions of Their Effects. Boundary Layer Effects in Turbomachines. AGARD AG-164, 1972, pp. 241-259.

26. Cebeci, Tuncer: Wall Curvature and Transition, Effects in Turbulent Boundary Layers. AIAA J., vol. 9, no. 9, Sept. 1971, pp. 1868-1870.

27. Turner, A.B.: Local Heat Transfer Measurements on a Gas Turbine Blade. J. Mech. Eng. Sci., vol. 13, no. 1, Feb. 1971, pp. 1-12.

28. Jaffe, N.A.; Okamura, T.T.; and Smith, A.M.O.: Determination of Spatial Amplification Factors and Their Application to Predicting Transition. AIAA J., vol. 8, no. 2, Feb. 1970, pp. 301-308.

29. Radbill, J.R.; and McCue, G.A.: Quasilinearization and Nonlinear Problems in Fluid and Orbital Mechanics. American Elsevier, New York, 1970.

30. Donaldson, Coleman du P.: A Computer Study of an Analytical Model of Boundary-Layer Transition. AIAA J., vol. 7, no. 2, Feb. 1969, pp. 271-278.

31. Tani, I.: Boundary Layer Transition. Annual Review of Fluid Mechanics, Vol. 1, W.R. Sears, ed., Annual Reviews Inc., 1969, pp. 169-196.

32. Knapp, C.F.; and Roache, P.J.: A Combined Visual and Hot-Wire Anemometer Investigation of Boundary Layer Transition. AIAA J., vol. 6, no. 1, Jan. 1968, pp. 29-36.

33. Schlichting, Hermann: The Origin of Turbulence. Boundary Layer Theory, 6th ed., McGraw-Hill, 1968.

34. Spangler, J.G.; and Wells, C.S.: The Effects of Free Stream Disturbances on Boundary Layer Transition. AIAA J., vol. 6, no. 3, Mar. 1968, pp. 543-545.

35. Obremski, H.J.; and Fejer, A.A.: Transition in Oscillating Boundary Layer Flows. J. Fluid Mech., vol. 29, part 1, July 18, 1967, pp. 93-111.

36. Squire, H.B.; and Johnston, W.D.: Measurements of Waviness of Wing Surfaces in Relation to Boundary Layer Transition. BR67826, Royal Aircraft Establishment, 1941.

37. Wells, C. Sinclair, Jr.: Effects of Free Stream Turbulence on Boundary Layer Transition. AIAA J., vol. 5, no. 1, Jan. 1967, pp. 172-174.

38. Bradshaw, P.: The Effect of Wind-Tunnel Screens on Nominally Two-Dimensional Boundary Layers. J. Fluid Mech., vol. 22, part 4, Aug. 1965, pp. 679-687.

39. Coles, Donald: Transition on Circular Couette Flow. J. Fluid Mech., vol. 21, part 3, Mar. 1965, pp. 386-425.

40. Goldstein, S.: Modern Developments in Fluid Dynamics. Dover, New York, 1965.

41. Van Driest, E.R.; and Blumer, C.B.: Boundary Layer Transition: Free-Stream Turbulence and Pressure Gradient Effects. AIAA J., vol. 1, no. 6, June 1963, pp. 1303-1306.

42. Rosenhead, L.: Laminar Boundary Layers. Clarendon Press, Oxford, 1963.

43. Coles, D.: Turbulent Boundary Layer in a Compressible Fluid. R-403-PR, Rand Corp., 1962, Appendix A.

44. Klebanoff, P.S.; Tidstrom, K.D.; and Sargent, L.M.: The Three-Dimensional Nature of Boundary-Layer Instability. J. Fluid Mech., vol. 12, part 1, Jan. 1962, pp. 1-34.

45. Lees, Lester; and Reshotko, Eli: Stability of the Compressible Laminar Boundary Layer. J. Fluid Mech., vol. 12, part 4, Apr. 1962, pp. 555-590.

46. Lin. C.C.; and Benny, D.J.: On the Instability of Shear Flows and Their Transition to Turbulence. Applied Mechanics, Proceedings of the 11th International Congress on Applied Mechanics, Henry Gortler, ed., Springer-Verlag, Berlin, 1966, pp. 797-802.

47. Tani, I.: Some Aspects of Boundary Layer Transition at Subsonic Speeds. Advances in Aeronautical Sciences, Vol. 3, Pergamon Press, New York, London, 1962, pp. 143-160.

48. Benney, D.J.; and Lin, C.C.: On the Secondary Motion Induced by Oscillation in a Shear Flow. Phys. Fluids, vol. 3, no. 4, July-Aug. 1960, pp. 656-657.

49. Elder, J.W.: An Experimental Investigation of Turbulent Spots and Breakdown to Turbulence. J. Fluid Mech., vol. 9, part 2, Oct. 1960, pp. 235-246.

50. Gibbings, J.C.: Aeronautical Research Council Current Paper 462, 1959.

51. Bergh, H.: A Method for Visualizing Periodic Boundary Layer Phenomena. Boundary Layer Research, H. Gortler, ed., Springer-Verlag, Berlin, 1958, pp. 173-178.

52. Dhawan, S.; and Narasimha, R.: Some Properties of Boundary Layer Flow During the Transition from Laminar to Turbulent Motion. J. Fluid Mech., vol. 3, no. 4, Jan. 1958, pp. 418-440.

53. Morkovin, M.V.: Transition from Laminar to Turbulent Shear Flow - A Review of Some Recent Advances in Its Understanding. Trans. ASME, vol. 80, July 1958, pp. 1121-1128.

54. Schubauer, G.B.; and Klebanoff, P.S.: Mechanism of Transition at Subsonic Speeds. Boundary Layer Research, H. Gortler, ed., Berlin, 1958, pp. 84-107.

55. Lin, C.C.: The Theory of Hydrodynamic Stability. Cambridge Univ. Press, 1955.

56. Schubauer, G.B.; and Klebanoff, P.S.: Contributions on the Mechanics of Boundary Layer Transition. NACA TN-3489, 1955.

57. Jedlicka, James R.; Wilkins, Max E.; and Seiff, Alvin: Experimental Determination of Boundary-Layer Transition on a Body of Revolution at M = 3.5. NACA TN-3342, 1954.

58. Stuart, J.T.: On the Stability of Viscous Flow Between Parallel Planes in the Presence of a Co-planar Magnetic Field. Proc. Roy. Soc., London, A, vol. 221, no. 1145, Jan. 21, 1954, pp. 189-206.

59. Granville, P.S.: The Calculations of Viscous Drag of Bodies of Revolution. Navy Dept., The David Taylor Model Basin, Report 849, 1953.

60. Emmons, H.W.: The Laminar-Turbulent Transition in a Boundary Layer - Part I. J. Aeronaut. Sci., vol. 18, no. 7, July 1951, pp. 490-498.

61. Prandtl, L.: Essentials of Fluid Dynamics. Hafner, New York, 1952.

62. Eckert, E.R.G.: Interferometric Studies on the Stability and Transition to Turbulence of a Free-Convection Boundary Layer. Proceedings of the General Discussion on Heat Transfer, Inst. Mech. Eng., London, 1951.

63. Goertler, N.: The Effect on Transition of Isolated Surface Excrescences in the Boundary Layer. R. & M. No. 2779, British A.R.C., 1951.

64. Eckert, Ernst R.G.: Interferometric Studies of Beginning Turbulence in Free and Forced Convection Boundary Layers on a Heated Plate. Heat Transfer and Fluid Mechanics Institute, ASME, 1949, pp. 181-190.

65. Dryden, Hugh L.: Recent Advances in the Mechanics of Boundary Layer FLow. Advances in Applied Mechanics, Vol. 1, Richard von Mises and Theodore Von Karman, eds., Academic Press, New York, 1948, pp. 1-40.

66. Liepmann, Hans W.; and Fila, Gertrude H.: Investigations of Effect of Surface Temperature and Single Roughness Elements on Boundary Layer Transition. NACA TN-1196, 1947.

67. Schubauer, G.B.; and Skramstad, H.K.: Laminar-Boundary-Layer Oscillations and Stability of Laminar Flow. J. Aeronaut. Sci., vol. 14, no. 2, Feb. 1947, pp. 69-78.

68. Liepmann, H.W.: Investigation of Boundary Layer Transition on Concave Walls. NACA Wartime Report W-87, 1945.

69. Liepmann, Hans W.: Investigations on Laminar Boundary-Layer Stability and Transition on Curved Boundaries. NACA Wartime Report W-107, 1943.

70. Dryden, Hugh L.: Turbulence and the Boundary Layer. J. Aeronaut. Sci., vol. 6, no. 3, Jan. 1939, pp. 85-105.

71. Goldstein, S.: On the Stability of Superposed Streams of Fluids of Different Densities. Proc. Roy. Soc., London, A, vol. 132, no. 820, Aug. 1, 1939, pp. 524-547.

72. Hall, A.A.; and Hislop, G.S.: Experiments on the Transition of the Laminar Boundary Layer on a Flat Plate. R. & M. No. 1843, British A.R.C., 1938.

73. Clauser, Milton; and Clauser, Francis: The Effects of Curvature on Transition from Laminar to Turbulent Boundary Layer. NASA TM-79878, 1937.

74. Dryden, Hugh L.: Air Flow in the Boundary Layer Near a Plate. NACA Report 562, 1936.

75. Dryden, H.L.: Boundary Layer Flow near Flat Plates. Proceedings, Fourth International Congress for Applied Mechanics, Cambridge, England, 1934, p. 175.

76. Von Karman, T.: Some Aspects of the Turbulence Problem. Proceedings, Fourth International Congress for Applied Mechanics, Cambridge, England, 1934, p. 54.

77. Taylor, G.I.: Internal Waves and Turbulence in a Fluid of Variable Density. Rapp. Proc. Verb. Cons. Internat. pour 1-Exploration de la Mer. LXXVI Copenhagen, 1931, pp. 35-42.

78. Taylor, G.I.: Effects of Variation in Density on the Stability of Superposed Streams of Fluid. Proc. Roy. Soc., London, A, vol. 132, no. 820, Aug. 1, 1931, pp. 499-523.

79. Burgers, J.M.: The Motion of a Fluid in the Boundary Layer along a Plane Smooth Surface. Proceedings, First International Congress for Applied Mechanics, Delft, 1924, p. 113.

80. Rayleigh, Lord: On the Stability of Certain Fluid Motions. Proc. London Math. Soc. 11, 57 (1880) and 19, 67 (1881); Scientific Papers I, 474-487; III, 17: IV, 203 (1895); and VI, 97 (1913).

81. Klebanoff, P.S.; and Tidstrom, K.D.: Evolution of Amplified Waves Leading to Transition in a Boundary Layer with Zero Pressure Gradient. NASA TN D-195, 1959.

82. Crabtree, L.F.: Prediction of Natural Transition in the Boundary Layer on an Aerofoil. J.R. Aeronaut. Soc., vol. 62, no. 571, July 1958, pp. 525-528.

83. Preston, E.J.: Prediction of Transition in the Boundary Layer on an Aerofoil. J.R. Aeronaut. Soc., vol. 62, no. 576, Dec. 1958, p. 901.

84. Smith, A.M.O.; and Giamberoni, N.: Transition, Pressure Gradient and Stability Theory. Proc. Ninth Int. Congr. Appl. Mech., Wiley, 1956.

85. Van Ingen, J.L.: A Suggested Semi-empirical Method for the Calculation of the Boundary Layer Transition Region. Report Nos. V.T.H. 71 and V.T.H. 74, Delft, Holland, 1956.

86. Fage, A.; and Preston J.H.: On Transition from Laminar to Turbulent Flow in the Boundary Layer. Proc. R. Soc., London, A., vol. 178, no. 973, June 12, 1941, pp. 201-227.

87. Dyban, Ye. P.; Epik, E. Ya.; and Suprun, T.T.: Characteristics of the Laminar Boundary Layer in the Presence of Elevated Free-Stream Turbulence. Fluid Mech. - Sov. Res., vol. 5, no. 4, July-Aug. 1976, pp. 30-36.

88. Blair, M.F.: Influence of Free-Stream Turbulence on Boundary Layer Transition in Favorable Pressure Gradients. J. Eng. Power, vol. 104, no. 4, Oct. 1982, pp. 743-750.

89. Blair, M.F.: Influence of Free-Stream Turbulence on Turbulent Boundary Layer Heat Transfer and Mean Profile Development, Part I - Experimental Data, Part II - Analysis of Results. J. Heat Transfer, vol. 105, no. 1, Feb. 1983, pp. 33-47.

90. Kachanov, Yu. S.; and Levchenko, V. Ya.: The Resonant Interaction of Disturbance at Laminar-Turbulent Transition in a Boundary Layer. J. Fluid Mech., vol. 138, Jan. 1984, pp. 209-247.

91. Simon, T.W.; and Moffat, R.J.: Turbulent Boundary Layer Heat Transfer Experiments: A Separate Effects Study on a Convexly Curved Wall. J. Heat Transfer, vol. 105, no. 4, Nov. 1983, pp. 835-840.

92. Chen, Karl, K.; and Thyson, Noel A.: Extension of Emmon's Spot Theory to Flows on Blunt Bodies. AIAA J., vol. 9, no. 5, May 1971, pp. 821-825.

93. Brown, A.; and Burton R.C.: The Effects of Free-Stream Turbulence Intensity and Velocity Distribution on Heat Transfer to Curved Surfaces. ASME Paper 77-GT-48, 1977.

94. Hylton, L.D., et al.: Analytical and Experimental Evaluation of the Heat Transfer Distribution over the Surfaces of Turbine Vanes. (EDR-11209, Detroit Diesel Allison; NASA Contract NAS3-22761.) NASA CR-168015, 1983.

95. Daniels, L.D.; and Browne, W.B.: Calculation of Heat Transfer Rates to Gas Turbine Blades. Int. J. Heat Mass Transfer, vol. 24, no. 5, May 1981, pp. 871-879.

96. Reshotko, Eli: Stability Theory as a Guide to the Evaluation of Transition Data. AIAA J., vol. 7, no. 6, June 1969, pp. 1086-1091.

97. Narasimha, Roddam: On the Distribution of Intermittency in the Transition Region of a Boundary Layer. J. Aeronaut. Sci., vol. 24, no. 9, Sept. 1957, pp. 711-712.

98. Higgins, W. Robert; and Pappas, Constantine C.: An Experimental Investigation of the Effect of Surface Heating on Boundary Layer Transition on a Flat Plate in Supersonic Flow. NACA TN-2351, 1951.

99. Van Driest, E.R.; and Boison, J. Christopher: Experiments in Boundary Layer Transition at Supersonic Speeds. J. Aeronaut. Sci., vol. 24, no. 12, Dec. 1957, pp. 885-899.

100. Mack, L.M.: Notes on the Theory of Instability and Incompressible and Compressible Laminar Boundary Layers. Von Karman Institute for Fluid Dynamics, Brussels, Belgium, 1968.

101. Markovin, M.V.: Critical Evaluation of Transition from Laminar to Turbulent Shear Layers with Emphasis on Hypersonically Traveling Bodies. AFFDL TR-68-149, Martin Marietta Corp., 1983. (AD-686178.)

102. Keltner, G.: Spatial Stability and Transition in Compressible Flat Plate Flows. Ph.D. Thesis, UCLA, 1973.

103. Taghavi, H.: Three-Dimensional Spatial Stability and Transition of Compressible Boundary Layer Flows. Ph.D. Thesis, UCLA, 1977.

104. Deem, R.E.; and Murphy, J.S.: Flat Plate Boundary Layer Transition at Hypersonic Speeds. AIAA Paper 65-128, 1965.

105. Richards, B.E.; and Stollery, J.L.: Transition Reversal on a Flat Plate at Hypersonic Speeds. Recent Developments in Boundary Layer Research, AGARDograph 97, 1965.

106. Shutz, N.W.: Free-Flight Boundary Layer Transition Investigations at Hypersonic Speeds. AIAA Paper 65-127, 1965.

107. Mack, L.M.: On the Application of Linear Stability Theory to the Problem of Supersonic Boundary-Layer Transition. AIAA Paper 74-134, 1974.

108. Dunn, D.W.; and Lin, C.C.: On the Stability of the Laminar Boundary Layer in a Compressible Fluid. J. Aeronaut. Sci., vol. 22, no. 7, July 1955, pp. 455-477.

109. Wazzan, A.R.; and Taghavi, H.: The Effect of Heat Transfer on Three-Dimensional Spatial Stability and Transition of Flat Plate Boundary Layer at Mach 3. Int. J. Heat Mass Transfer, vol. 25, no. 9, Sept. 1982, pp. 1321-1331.

110. Eppler, R.; and Fasel, H.: Laminar-Turbulent Transition. Springer-Verlag, Berlin, 1980.

(a) Blasius boundary layer.
(b) Accelerating boundary layer.
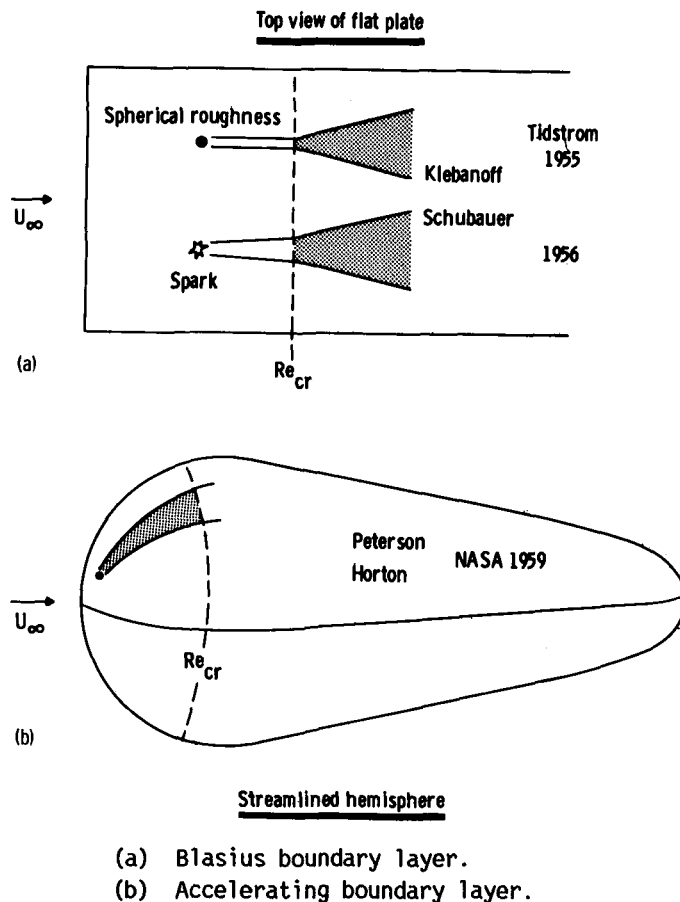
Figure 1. – Growth of turbulent wedges in relation to critical Reynolds number Re_{cr} for growth of infinitesimal disturbances in a Blasius and an accelerating boundary layer.

a

Horseshoe vortex H

Smoke Layer

H

Cylinder

S

b

S'

Spiral smoke filaments

A — — — A

c

Smoke layer →

Surface →

H   H

Dry regions of china clay

Section A-A
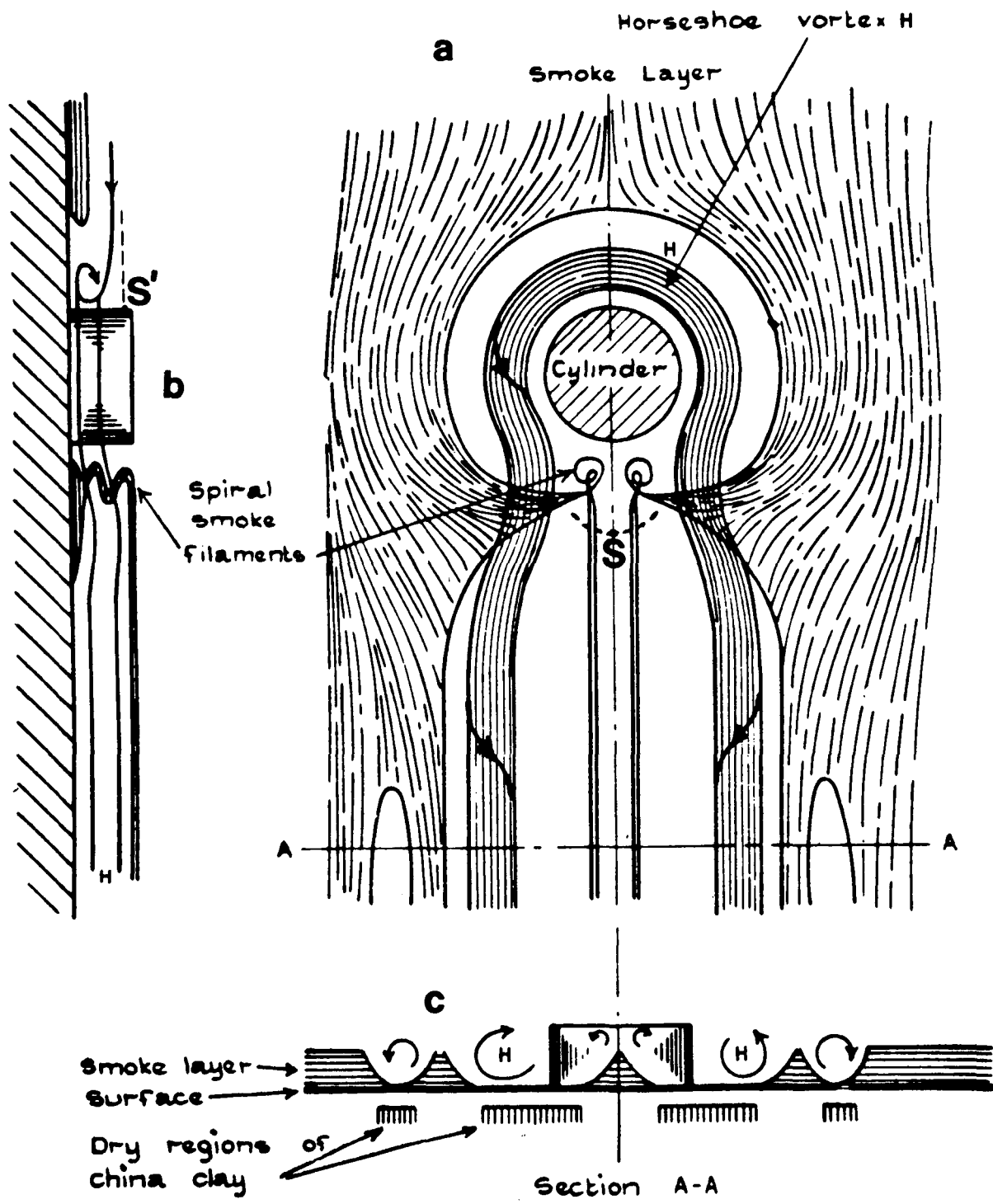
(a) Top view.   (b) Side view.   (c) Rear view.

Figure 2. – Schematic of features in second steady stage of flows around cylindrical protuberances, as visualized by Gregory and Walker (ref. 12).
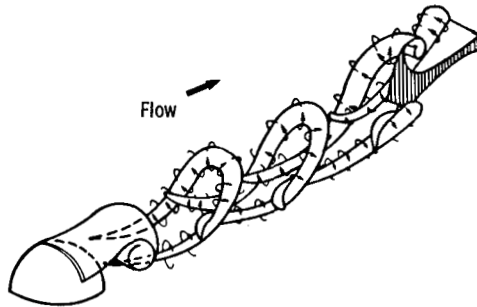
Figure 3. – Schematic of periodic hairpin–vortex formation downstream of hemisphere protuberance, as visualized by C.R. Smith for Re_k in range 450 to 550. At the wake edges these vortices interact with the two arms of a counterrotating horseshoe vortex wrapped around the front of the hemisphere (not shown).
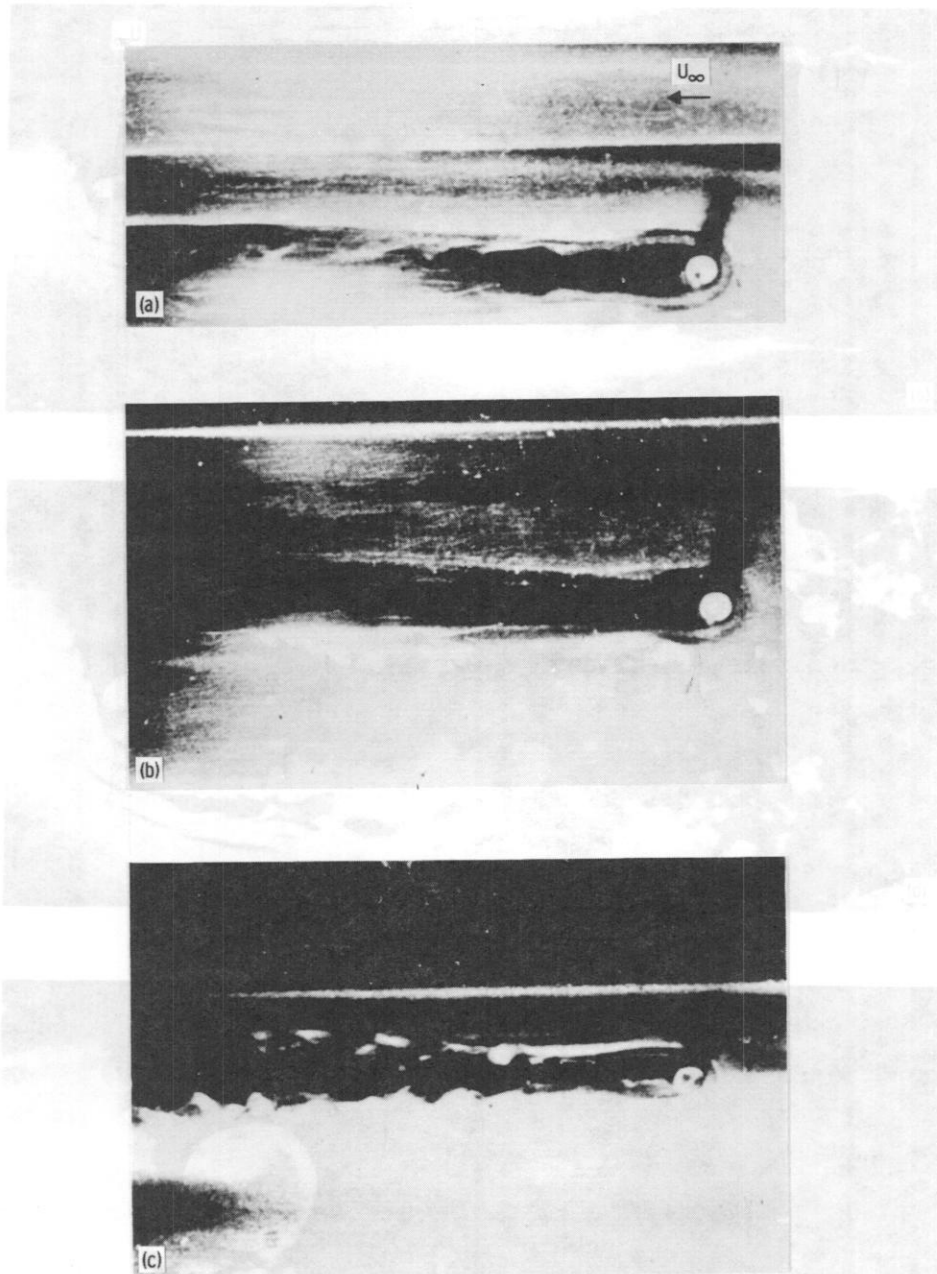
(a) Laminar wake: $U_\infty = 7$ ft/sec; $k = 0.188$ in; $\delta = 0.3$ in; $Re_k = 610$.
(b) Periodic disturbances: $U_\infty = 9.5$ ft/sec; $k = 0.188$ in; $\partial = 0.25$ in; $Re_k = 890$.
(c) Turbulent wedge forming near cylinder: $U_\infty = 18.3$ ft/sec; $k = 0.188$ in; $\delta = 0.18$ in; $Re_k = 1800$.

Figure 4. – Smoke visualization of vorticity rearrangement at fixed cylinder that protrudes into thinning boundary layer as external speed increases. (From ref. 13.)
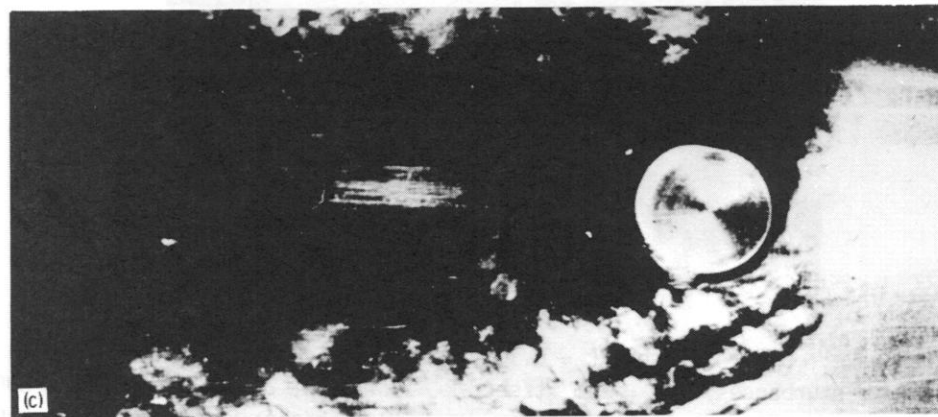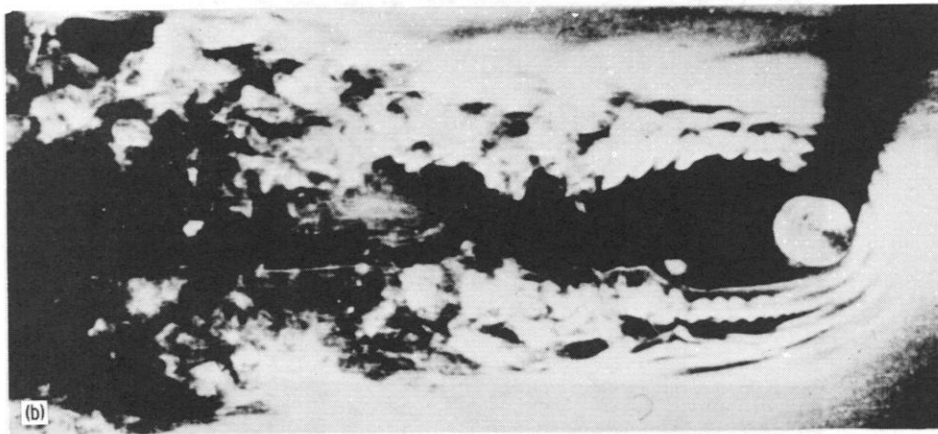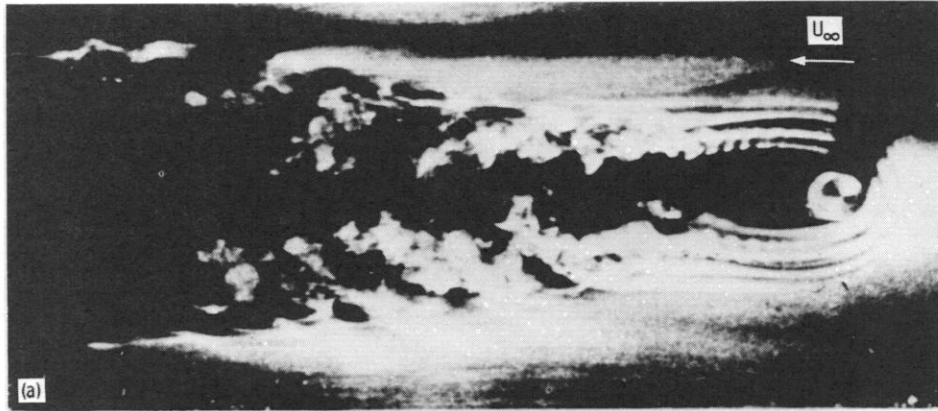
(a) Horseshoe system oscillation beginning: $k = 0.375$ in; $\delta = 0.18$ in; $Re_k = 3600$.
(b) Horseshoe system oscillating strongly: $k = 0.5$ in; $\delta = 0.18$ in; $Re_k = 4800$.
(c) Horseshoe system turbulent upstream of trip: $k = 1.0$ in; $\delta = 0.18$ in; $Re_k = 9600$.

Figure 5. – Smoke visualization (at fixed external speed) of new instabilities in boundary layer distorted by cylinders with $k = D$, as these protrude further outward. $U_\infty = 18.3$ ft/sec. (From ref. 13.)

PLAN VIEW

SIDE VIEW

$\sigma = \dfrac{d}{M}$

Figure 6. – Schematic of vortex flow module proposed for augmentation of heat transfer from bluff bodies.
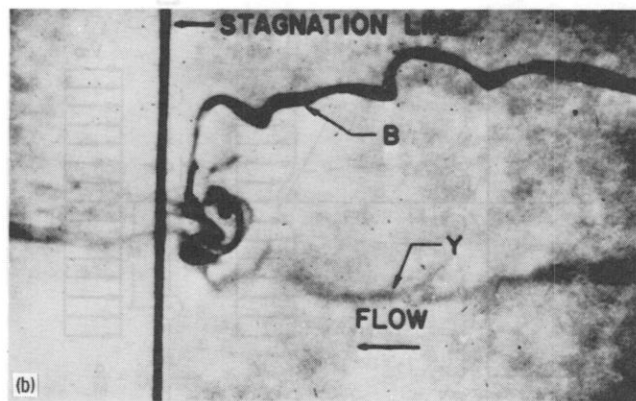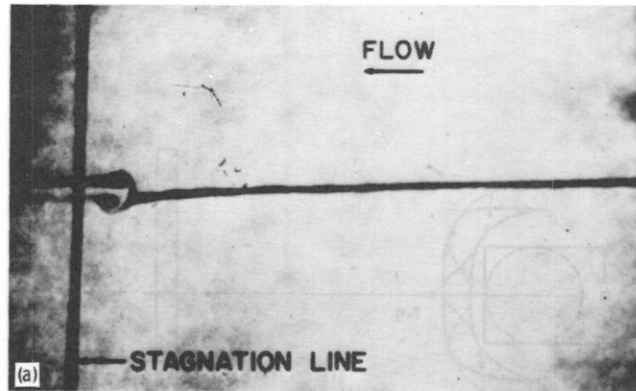
(a) Re_d = 30; Re_D = 1040; $\Delta x/d$ = 111; d = 0.027 in; D = 0.935 in.
(b) Re_d = 365; Re_D = 2730; $\Delta x/d$ = 32; d = 0.125 in; D = 0.935 in.

Figure 7. – Side-view dye visualization of single wake impinging on rectangular cylinder at Re_d of 30 and 365. (From ref. 14.)
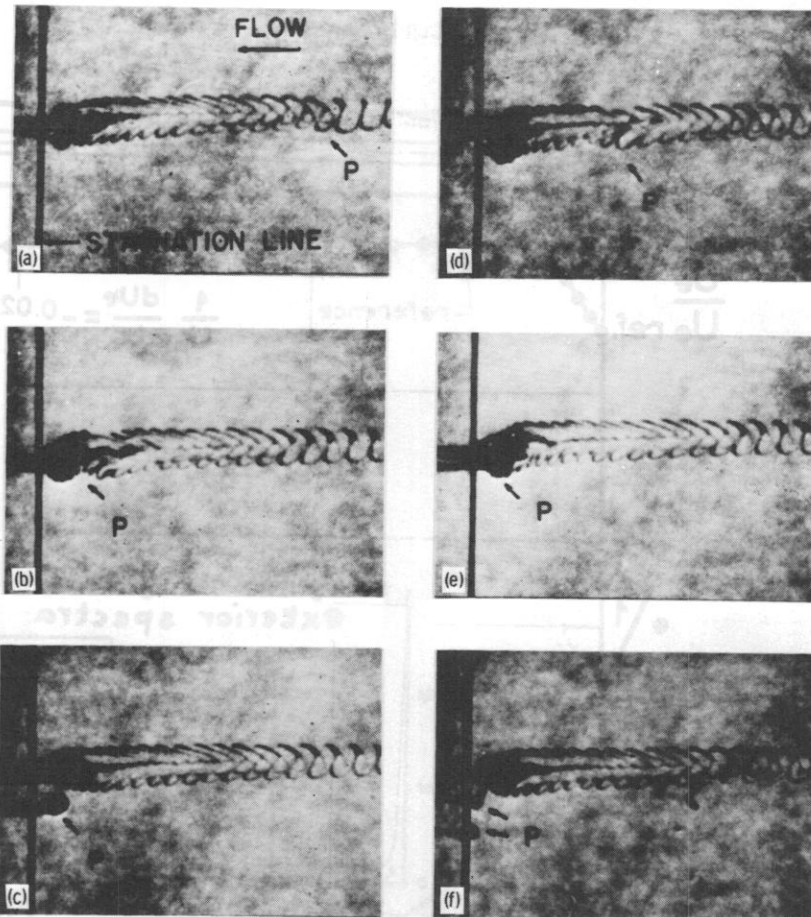
(a) t = 0.   (d) t = 0.34 sec.
(b) t = 0.14 sec.   (e) t = 0.44 sec.
(c) t = 0.24 sec.   (f) t = 0.55 sec.

Figure 8. – Side-view dye visualization showing effect of free-stream perturbation P on vortex flow module at $Re_d = 90$.
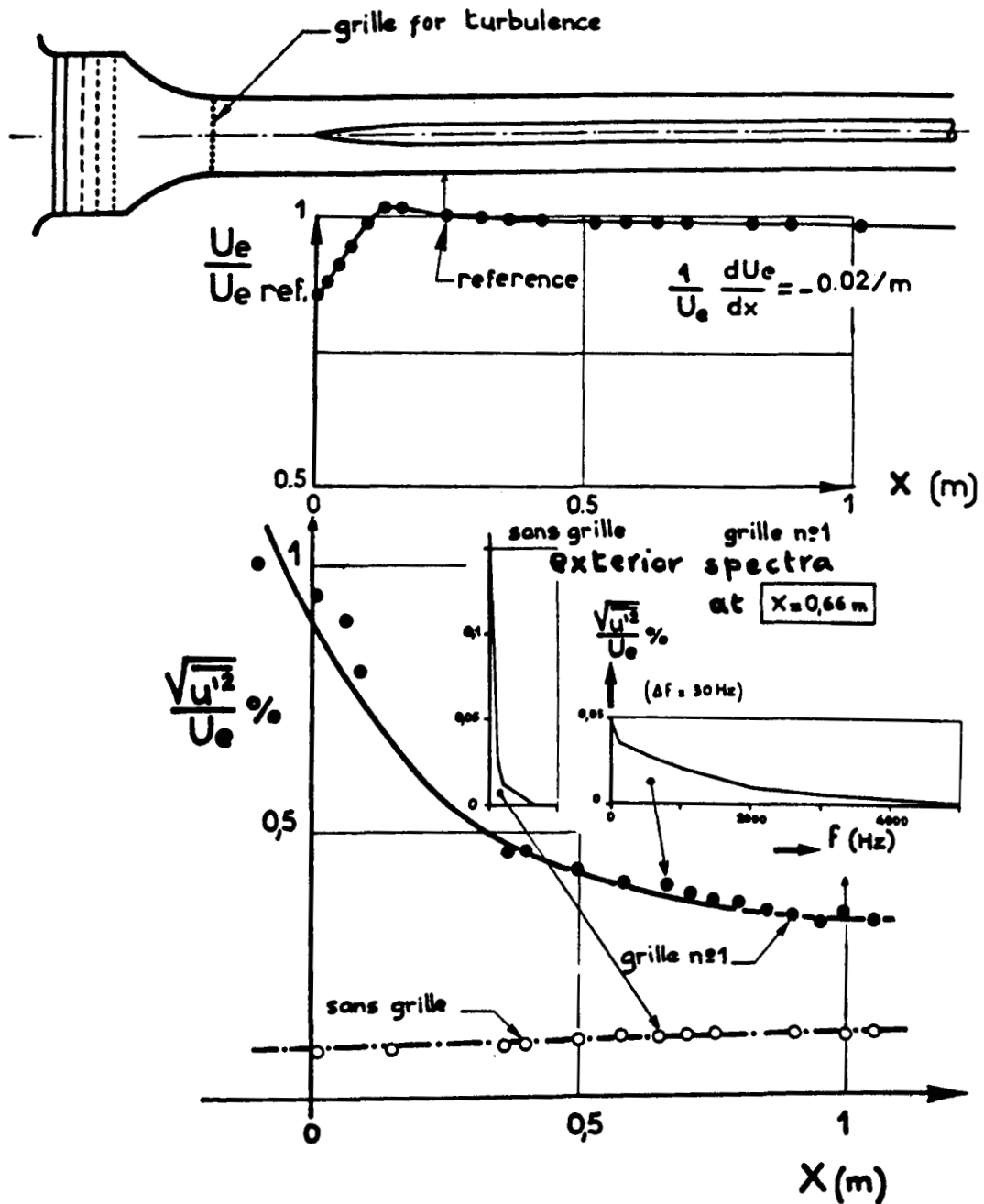
Figure 9. - Turbulence development and sample spectra outside boundary layer along axisymmetric slender body with and without upstream grid. (From ref. 17.)
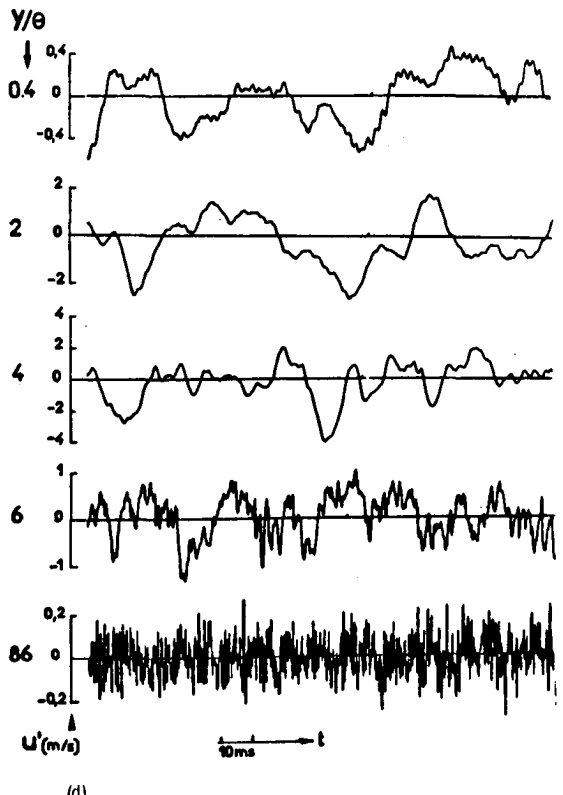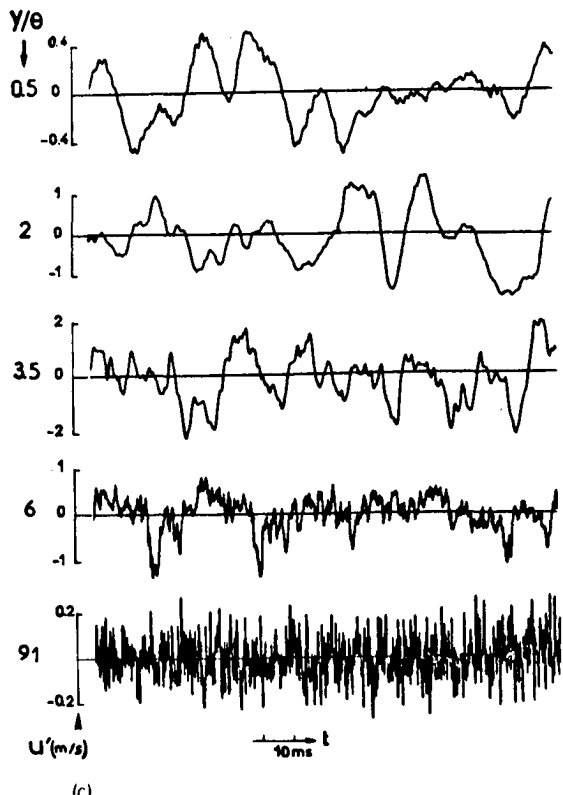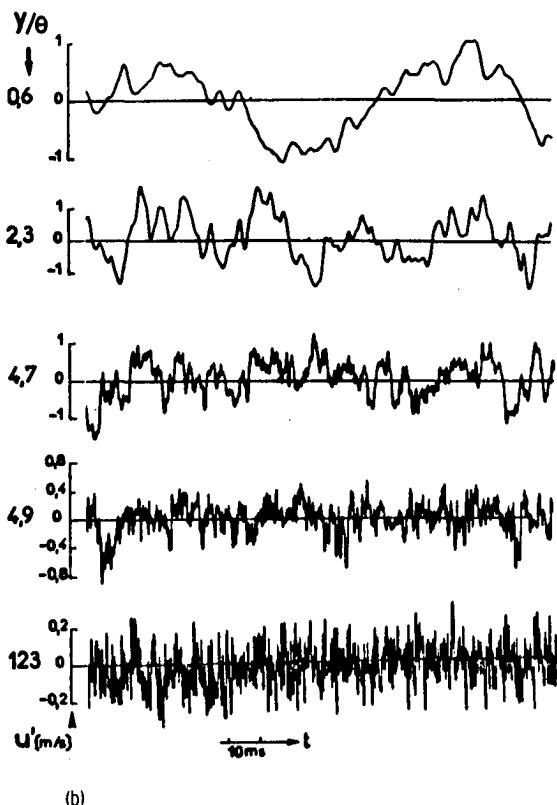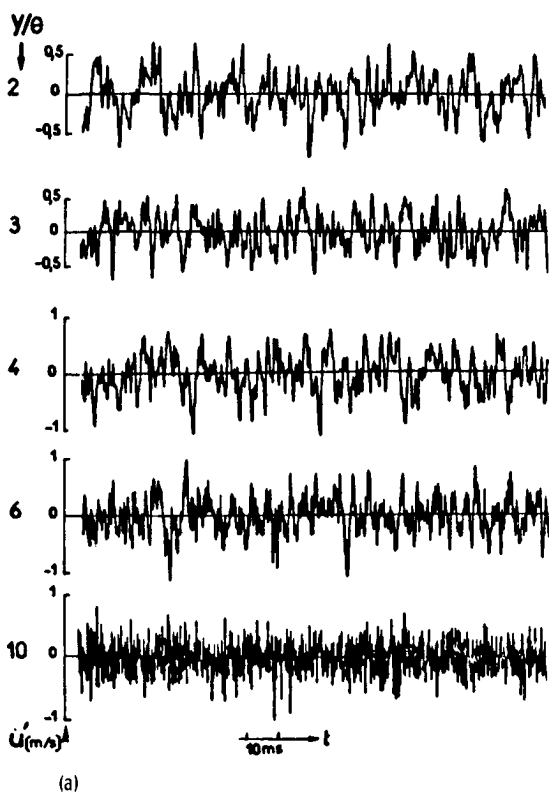
(a) x = 3.7 cm.   (b) x = 36 cm.
(c) x = 66 cm.   (d) x = 85 cm.

Figure 10. – Samples of fluctuations u(t) at five heights y of laminar boundary layer growing
in presence of grid at x of 3.7, 36, 66, and 85 cm. (From ref. 17.)

Characteristics of the Laminar Boundary Layer in the Presence of Elevated Free-Stream Turbulence

YE.P. DYBAN, E.YA. EPIK AND T.T. SUPRUN

The behavior of the laminar boundary layer was observed at free-stream turbulence of 0.3 to 25.2%. The increases in the boundary layer thickness, in the tangential stress at the wall, and in the momentum thickness with increase in turbulence are estimated. It is shown that the depth to which the fluctuations penetrate into the boundary layer does not depend on the turbulence but only on the Reynolds number. The perturbation peak in the layer are highest at free-stream turbulence of the order of 4.5%. The longitudinal scale of turbulence increases monotonically toward the outer edge of the layer, while its spectral distributions exhibit low (less than 300 Hz) frequencies.
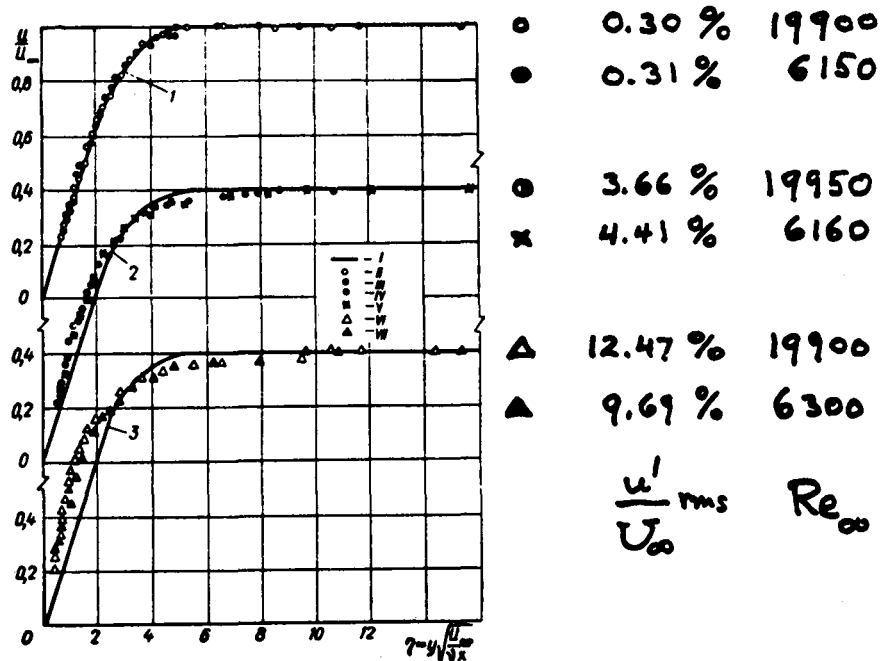
Fig. 1. Velocity distribution in the laminar boundary layer.

Figure 11. – Abstract and mean laminar boundary-layer profiles in presence of increasing free-stream turbulence. (From ref. 22.)

Characteristics of the Laminar Boundary Layer in the Presence of Elevated Free-Stream Turbulence

YE. P. DYBAN, E. YA. EPIK AND T. T. SUPRUN

Do Q
$\mathcal{L}/\delta^*$

The behavior of the laminar boundary layer was observed at free-stream turbulence of 0.3 to 25.2%. The increases in the boundary layer thickness, in the tangential stress at the wall, and in the momentum thickness with increase in turbulence are estimated. It is shown that the depth to which the fluctuations penetrate into the boundary layer does not depend on the turbulence but only on the Reynolds number. The perturbation peak in the layer are highest at free-stream turbulence of the order of 4.5%. The longitudinal scale of turbulence increases monotonically toward the outer edge of the layer, while its spectral distributions exhibit low (less than 300 Hz) frequencies.
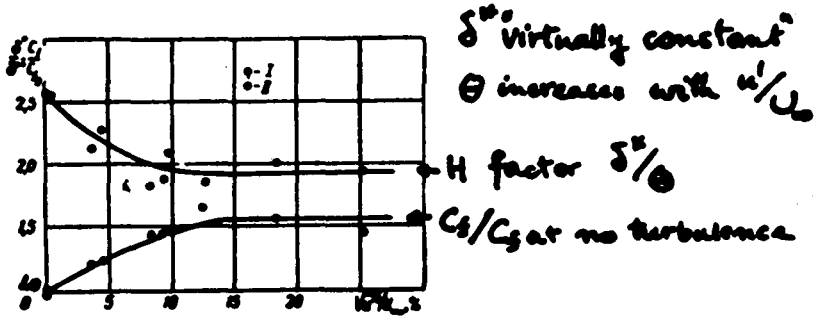
30°
Thickness not given.

δ^{**} "virtually constant"
Θ increases with u'/U_0
H factor δ^*/Θ
C_f/C_{f_0} at no turbulence

Fig. 2. Variation in drag coefficient and form factor in the laminar layer.
I) c_f/c_{f_0}; II) δ^*/δ^{**}.

25.2%
18.4%
9.49%
4.91%
0.31%

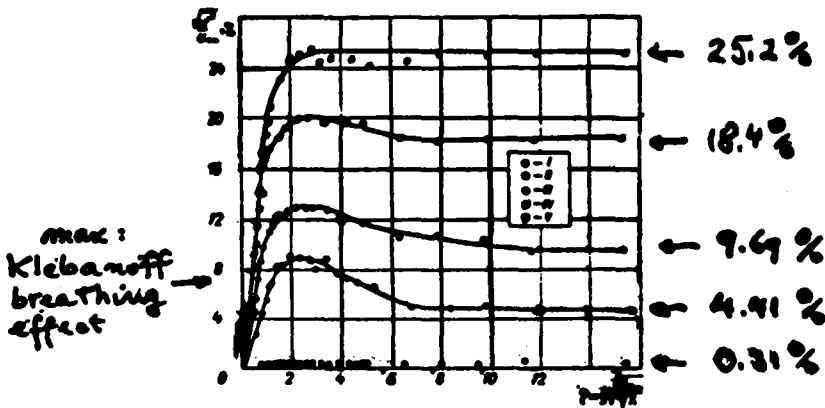*max: Klebanoff breathing effect*

Fig. 3. Distribution of fluctuations in the laminar layer at $Re_x \approx 6.2 \cdot 10^3$. *6200*

Figure 12. – Variation of skin friction ratio, shape factor, and u' fluctuation profiles in a laminar boundary layer as free-stream turbulence increases. (From ref. 22.)

FLuid turbulence is 100 years old,

still not understood → in application:
(all around us)

↘ no basic Theory

altho we have known the
basic NAVIER-STOKES EQs
all along ....

nonlinear   Partial D.E's in x,y,z,t

↘ too
much
Coefficient of highest derivative   "freedom"
Very small (F.M. → singular   as speed
perturbations)   ∪ ↑
Very Sensitive to small
changes in initial conditions as Re↑

<u>Key syndromes</u> of <u>TURBULENT STATES</u>:

1 irregularity (disorder)   → stochastic Non·Lin.
partial   systems

2 3·DIM vorticity (eddying) → ensemble of loosely
coupled deformable
gyroscopes: SURPRISES!

3 diffusion far in excess   → both friend and
of molecular <u>mixing</u>   foe
4 dissipation — scale changes   on a large range
in x or t   of scales, large to small
↘ broad-band spectra

① represents strange behavior in
continuum mechanics
↳ apparently common in NONLIN.DISS.SYSTEMS with larger number
"strange attractors"   of degrees of freedom

Figure 13. – Salient features of turbulence.
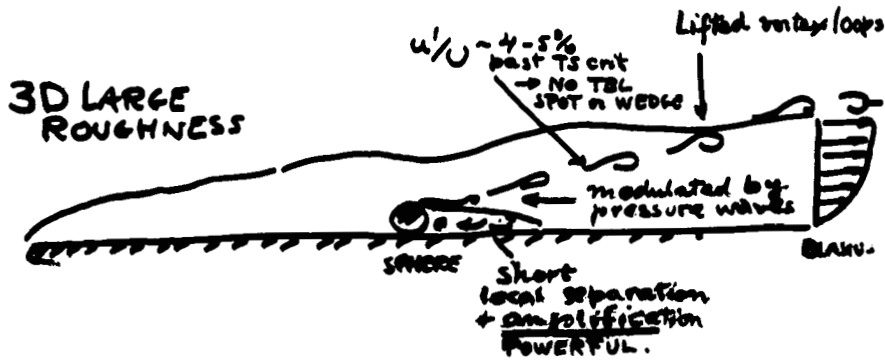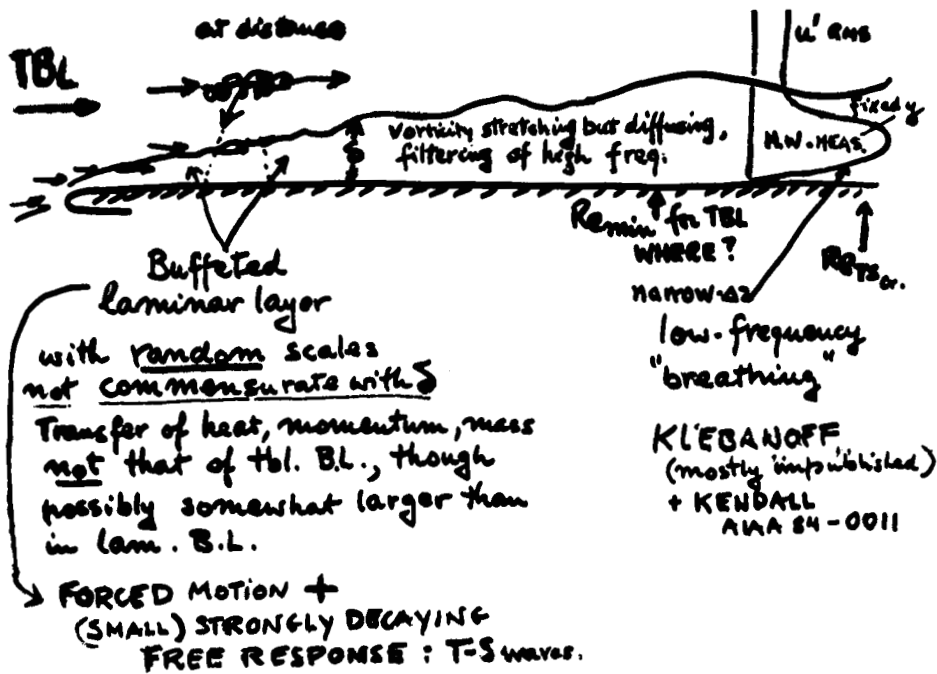
Figure 14. — Schematic of influence on growing laminar boundary layer of external turbulence (top) and a three-dimensional protuberance (bottom).
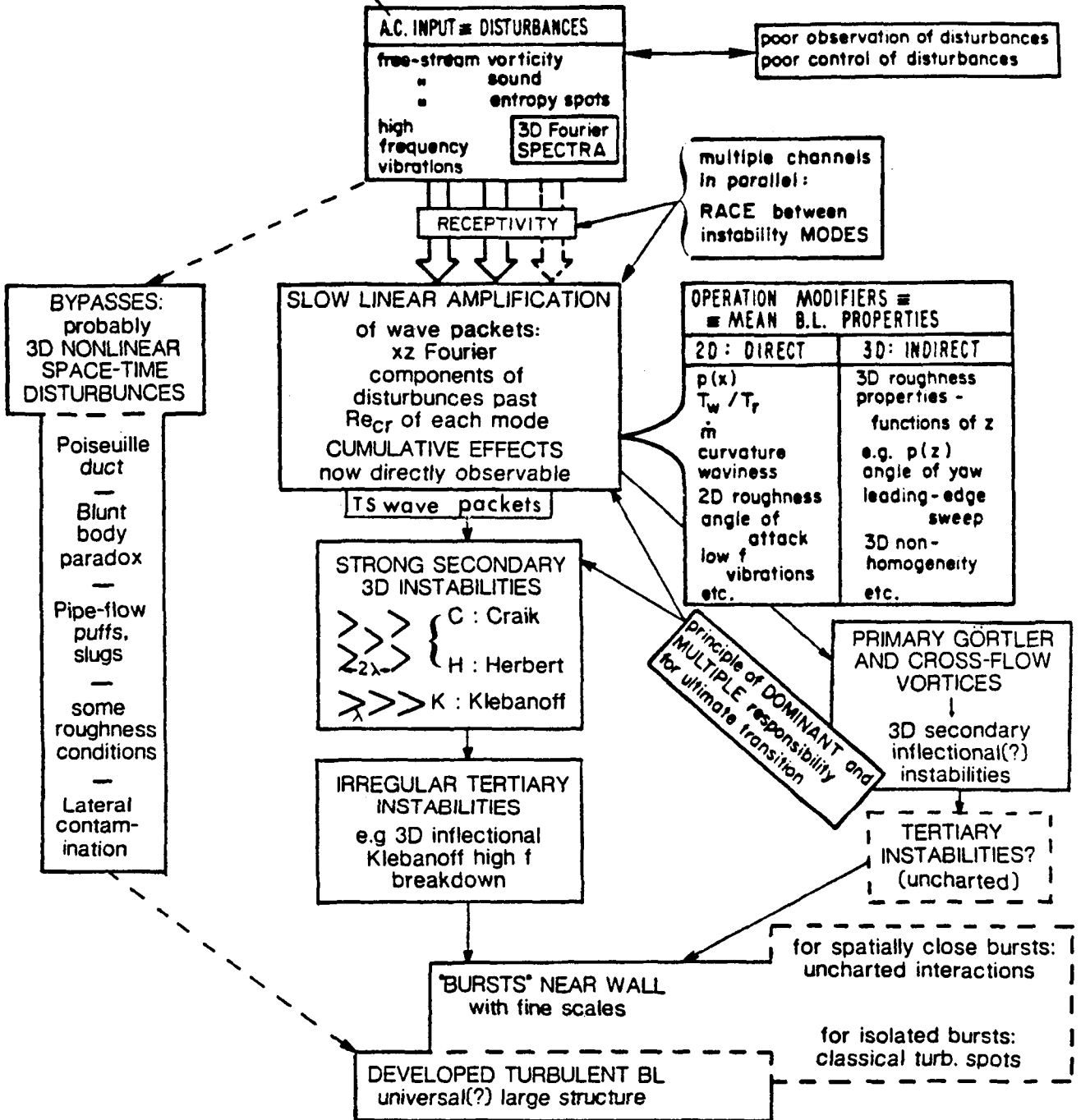
Figure 15. – Evolutionary paths to turbulence in undistorted boundary layers and ducts for mild environmental disturbances – 1984.